Room-Temperature Suzuki-Miyaura Polycondensation of Aryl Dichloride Monomers Enabled by "Large-but-Flexible" Pd-NHC Precatalysts

Juan-Juan Feng,[†+] Yuman Guo,[†+] Qian Song,[†] Ze-Cheng Guo,[†] Feng-Shou Liu[†*]

[†]*School of Chemistry and Chemical Engineering, Guangdong Cosmetics Engineering and Technology Research Center, Guangdong, Pharmaceutical University, Zhongshan, Guangdong 528458, China*

Content of Supporting Information

1. Physical Measurements…….....S2

2. Experimental Procedure: General Procedure for the Synthesis of Pd-NHCs S3

3. NMR spectra for the products.....S9

4. The Optical Spectra: UV-Vis Absorption and Fluorescence Emission S29

5. GPC spectra for the products S32

6. DFT calculations of rotational barriers S43

7. References S46

1. Physical Measurements

NMR spectra were acquired on a Bruker DMX 400 MHz instrument at ambient temperature, using TMS as an internal standard and $CDCl_3$ as the solvent. Single-crystal X-ray diffraction data were collected using the ω-2θ scan mode on a Bruker SMART 1000 CCD diffractometer with graphite-monochromated Mo Kα radiation (λ = 0.71073 Å) at 173 K for compounds **C1, C2, C4** and **C5**. Cell parameters were refined globally based on the positions of all collected reflections. Intensities were corrected for Lorentz and polarization effects, as well as empirical absorption. Structures were solved by direct methods and refined using full-matrix least squares on F2. Hydrogen atoms were placed in calculated positions. Structure solution and refinement were performed using the SHELXL-97 software package. All non-hydrogen atoms were refined anisotropically, with hydrogen atoms introduced in calculated positions and displacement factors matching those of the host carbon atoms. GPC analyses of the molecular weights and molecular weight distributions (PDI = Mw/Mn) of the polymers were performed on a Waters Breeze 2 GPC chromatograph equipped with a differential refractive-index detector. Tetrahydrofuran (THF) used as the eluent at a flow rate of 1.0 mL/min.

2. Experimental Procedure: General Procedure for the Synthesis of Pd-NHCs

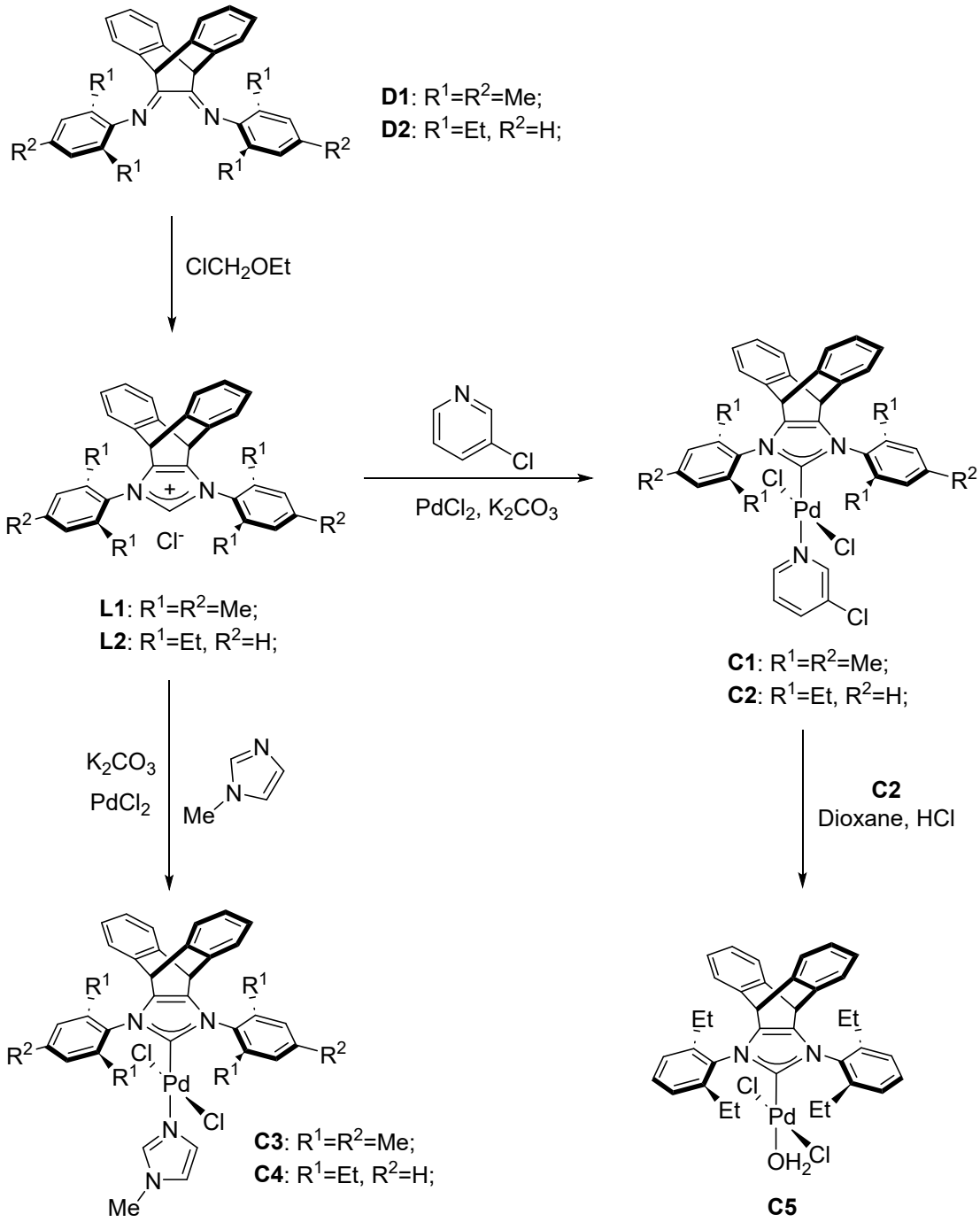

Sceheme **S1**. The synthetic routes for the Pd-NHCs

2.1 General Procedure for the Synthesis of Imidazolium Salts

The imidazolium salts of **L** were synthesized as following procedures: a mixture of α-diimine compound **D1** or **D2** (1.0 mmol) and chloromethyl ethyl ether (3 mL) was added to a thick-walled pressure tube and heated at 100 °C under a nitrogen atmosphere for 24 hours. Upon completion, the reaction mixture was cooled to room temperature, and anhydrous diethyl ether was added to induce precipitation. The resulting solid was collected by filtration and thoroughly washed with anhydrous diethyl ether (3 × 10 mL) to afford the imidazolium salt products of **L1** or **L2**.

L1 was obtained as white powder with a yield of 63%. ^{1}H NMR (400 MHz, $CDCl_3$) δ 10.57 (s, 1H), 7.53 (dd, *J* = 5.3, 3.2 Hz, 4H), 7.29 – 7.18 (m, 8H), 5.33 (s, 2H), 2.57 (s, 6H), 2.15 (s, 12H). ^{13}C NMR (101 MHz, $CDCl_3$) δ 144.2, 144.0, 141.3, 134.4, 129.9, 128.7, 126.2, 124.2, 45.8, 21.2, 17.7. HRMS (ESI^+): 481.2649 (calcd for $C_{35}H_{33}N_2$, $[M\text{-}Cl]^+$ 481.2644).

L2 was obtained as white powder with a yield of 90%. ^{1}H NMR (400 MHz, $CDCl_3$) δ 10.52 (s, 1H), 7.52 (t, *J* = 7.7 Hz, 2H), 7.31 (d, *J* = 7.5 Hz, 8H), 7.03 (dd, *J* = 5.4, 3.1 Hz, 4H), 5.14 (s, 2H), 2.24 (d, *J* = 7.6 Hz, 8H), 0.96 (t, *J* = 7.6 Hz, 12H). ^{13}C NMR (101 MHz, $CDCl_3$) δ 144.4, 143.8, 140.5, 133.7, 131.7, 129.9, 127.5, 126.2, 124.3, 45.9, 24.2, 14.3. HRMS (ESI^+): 509.2961 (calcd for $C_{37}H_{37}N_2$, $[M\text{-}Cl]^+$ 509.2957).

2.2 General Procedure for the Synthesis of Pd-NHCs (C1 and C2)

To a 100 mL nitrogen-purged round-bottom flask were added the imidazolium salt (1.0 mmol), $PdCl_2$ (1.1 mmol), K_2CO_3 (10 mmol), and 3-chloropyridine (1 equiv.). The

reaction mixture was stirred at 90 °C for 24 hours under an inert atmosphere. After cooling to ambient temperature, dichloromethane (20 mL) was added, and the mixture was filtered through a short pad of silica gel, washing thoroughly with additional dichloromethane to ensure complete elution of the product. The combined organic fractions were concentrated under reduced pressure to give a crude yellow solid. This solid was redissolved in a minimal volume of dichloromethane (*ca* 0.5 mL), followed by slow addition of n-hexane to induce precipitation. The resulting yellow powder was collected by filtration and dried under vacuum to afford the pure Pd-NHC complex.

C1 was obtained as light yellow powder with a yield of 70%. ^{1}H NMR (400 MHz, $CDCl_3$) δ 8.53 (d, *J* = 2.3 Hz, 1H), 8.44 (dd, *J* = 5.6, 1.4 Hz, 1H), 7.52 (ddd, *J* = 8.2, 2.4, 1.4 Hz, 1H), 7.23 (dd, *J* = 5.3, 3.2 Hz, 4H), 7.09 (s, 4H), 7.02 (dd, *J* = 8.2, 5.6 Hz, 1H), 6.94 (dd, *J* = 5.3, 3.1 Hz, 4H), 4.96 (s, 2H), 2.43 (s, 6H), 2.12 (s, 12H). ^{13}C NMR (101 MHz, $CDCl_3$) δ 150.4, 149.5, 145.9, 145.4, 139.3, 137.4, 136.7, 129.2, 125.3, 124.2, 123.7, 46.8, 31.6, 22.7, 21.3, 19.1, 14.1. HRMS (ESI^+): 734.1323 (calcd for $C_{40}H_{36}Cl_2N_3Pd$, $[M\text{-}Cl]^+$ 734.1321).

C2 was obtained as light yellow powder with a yield of 75%. ^{1}H NMR (400 MHz, $CDCl_3$) δ 8.42 (d, *J* = 2.3 Hz, 1H), 8.34 (dd, *J* = 5.6, 1.3 Hz, 1H), 7.59 – 7.46 (m, 3H), 7.37 (d, *J* = 7.7 Hz, 4H), 7.22 (dd, *J* = 5.3, 3.2 Hz, 4H), 7.04 – 6.88 (m, 5H), 5.01 (s, 2H), 2.72 (dq, *J* = 15.3, 7.6 Hz, 4H), 2.34 (dq, *J* = 15.0, 7.4 Hz, 4H), 1.06 (t, *J* = 7.5 Hz, 12H). ^{13}C NMR (101 MHz, $CDCl_3$) δ 151.0, 146.5, 143.2, 138.0, 130.7, 126.7, 125.9, 124.9, 124.6, 77.7, 47.7, 25.1, 14.8. HRMS (ESI^+): 762.1630 (calcd for $C_{42}H_{40}Cl_2N_3Pd$, $[M\text{-}Cl]^+$ 762.1634).

2.3 General Procedure for the Synthesis of Pd-NHCs (C3 and C4)

To a 100 mL nitrogen-purged round-bottom flask were added imidazolium salt (1.0 mmol), $PdCl_2$ (1.1 mmol), K_2CO_3 (10 mmol), and N-methylimidazole (1 equiv.). The reaction mixture was stirred at 60 °C for 6 hours under an inert atmosphere. After cooling to room temperature, dichloromethane (20 mL) was added, and the mixture was filtered through a short pad of silica gel, washing thoroughly with additional dichloromethane to ensure complete elution of the product. The combined organic fractions were concentrated under reduced pressure to afford a crude yellow solid. This solid was redissolved in a minimal volume of dichloromethane (*ca* 0.5 mL), followed by slow addition of n-hexane to induce precipitation. The resulting light yellow powder was collected by filtration and dried under vacuum to afford the Pd-NHC complexes.

C3 was obtained as light yellow powder with a yield of 25%. ^{1}H NMR (400 MHz, $CDCl_3$) δ 7.90 (d, *J* = 1.3 Hz, 1H), 7.48 – 7.38 (m, 5H), 7.36 (t, *J* = 1.4 Hz, 1H), 7.26 (s, 4H), 7.14 (dd, *J* = 5.4, 3.2 Hz, 4H), 5.13 (s, 2H), 3.62 (s, 3H), 2.60 (s, 6H), 2.34 (s, 12H). ^{13}C NMR (101 MHz, $CDCl_3$) δ 146.6, 145.7, 139.6, 139.0, 137.4, 133.7, 129.8, 129.0, 125.9, 124.3, 119.4, 47.4, 34.5, 21.9, 19.7. HRMS (ESI^+): 703.1819 (calcd for $C_{39}H_{38}ClN_4Pd$, $[M\text{-}Cl]^+$ 703.1820)

C4 was obtained as light yellow powder with a yield of 59%. ^{1}H NMR (400 MHz, $CDCl_3$) δ 7.62 (t, *J* = 1.3 Hz, 1H), 7.50 (t, *J* = 7.6 Hz, 2H), 7.33 (d, *J* = 7.7 Hz, 4H), 7.21 (dd, *J* = 5.3, 3.2 Hz, 4H), 7.08 (t, *J* = 1.3 Hz, 1H), 6.93 (dd, *J* = 5.4, 3.1 Hz, 4H), 6.47 (t, *J* = 1.6 Hz, 1H), 4.98 (s, 2H), 3.40 (s, 3H), 2.80 – 2.67 (m, 4H), 2.37 (dd, *J* = 15.6, 7.6 Hz, 4H), 1.05 (t, *J* = 7.6 Hz, 12H). ^{13}C NMR (101 MHz, $CDCl_3$) δ 144.9,

144.0, 141.5, 137.3, 128.7, 127.5, 124.9, 124.1, 122.8, 117.8, 46.0, 32.9, 23.4, 13.0. HRMS (ESI$^+$): 731.2136 (calcd for $C_{41}H_{42}ClN_4Pd$, [M-Cl]$^+$ 731.2133).

2.4 Synthesis Procedure of Pd-NHC of C5:

To a 100 mL round-bottom flask were added complex **C2** (1.0 mmol), aqueous HCl (1 mL), and 1,4-dioxane (10 mL). The reaction mixture was stirred at room temperature for 24 hours under ambient conditions. After completion, dichloromethane (20 mL) was added, and the resulting mixture was filtered through a short pad of silica gel, eluting thoroughly with additional dichloromethane. The combined organic fractions were concentrated under reduced pressure to afford a yellow solid. The crude product was redissolved in a minimal volume of dichloromethane (*ca* 0.5 mL), followed by slow addition of n-hexane to induce precipitation. The resulting light yellow powder was collected by filtration and dried under vacuum to afford the product in 32% yield. ^{1}H NMR (400 MHz, $CDCl_3$) δ 7.59 (t, *J* = 7.5 Hz, 4H), 7.41 (t, *J* = 7.1 Hz, 8H), 7.26 (td, *J* = 6.3, 5.3, 3.1 Hz, 8H), 6.99 (td, *J* = 5.4, 4.9, 2.6 Hz, 8H), 5.03 (d, *J* = 6.7 Hz, 4H), 2.72 (dp, *J* = 15.2, 7.5 Hz, 8H), 2.33 (dt, *J* = 15.6, 7.4 Hz, 8H), 1.10 (q, *J* = 7.3 Hz, 24H). ^{13}C NMR (101 MHz, $CDCl_3$) δ 145.8, 145.1, 142.4, 134.1, 130.0, 126.0, 125.2, 123.9, 47.0, 24.3, 13.9. HRMS (ESI$^+$): 510.3091 (calcd for $C_{37}H_{38}N_2$, [M-$PdCl_2$-H_2O]$^+$ 510.3035).

2.4 General experimental procedures for kinetic studies of model small-molecule SM cross-coupling reactions

2,6-Dichloropyrazine (M1, 0.2 mmol), phenylboronic acid (0.5 mmol), KOtBu (2 mmol), precatalyst (1 mol%), and a mixture of THF/H_2O (3:1, 4 mL) were added to a

reaction tube. The reaction was conducted at room temperature under a nitrogen atmosphere. Upon reaching the designated reaction time, the mixture was extracted and analyzed by gas chromatography (GC). Meanwhile, the intermediate products were isolated and purified by column chromatography, followed by characterization using NMR spectroscopy.

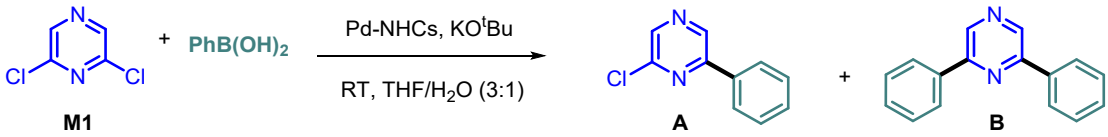

A: ^{1}H NMR (400 MHz, $CDCl_3$) δ 8.93 (s, 1H), 8.52 (s, 1H), 8.07 – 7.97 (m, 2H), 7.56 – 7.47 (m, 3H). ^{13}C NMR (101 MHz, $CDCl_3$) δ 152.6, 142.4, 139.3, 134.8, 130.6, 129.1, 127.1.

B: ^{1}H NMR (400 MHz, $CDCl_3$) δ 8.97 (s, 2H), 8.16 (dd, J = 7.5, 1.8 Hz, 4H), 7.52 (dd, J = 12.9, 7.2 Hz, 6H). ^{13}C NMR (101 MHz, $CDCl_3$) δ 151.6, 139.8, 136.5, 129.9, 129.0, 127.0.

2.5 General Procedure for Palladium-Catalyzed Suzuki-Miyaura Cross-Coupling Polycondensations

The dichlorinated compound (0.2 mmol), diboronic ester (0.2 mmol), KO^{t}Bu (0.8 mmol), precatalyst (1 mol%), and a mixture of THF/H_2O (3:1, 4 mL) were added to a reaction tube. The reaction was conducted at room temperature under a nitrogen atmosphere for 12 hours. Upon completion, methanol was added to precipitate the polymer, which was collected by vacuum filtration. The crude polymer was subsequently washed with water at 50 °C to remove residual base, followed by Soxhlet

extraction with n-hexane to eliminate small-molecule oligomers. The resulting polymer was dried under vacuum to afford the purified product.

2.6 General Procedure for Palladium-Catalyzed chemoselective Suzuki-Miyaura Cross-Coupling :

2,7-Dibromo-9H-carbazole (2 mmol), 3-(bromomethyl)heptane (5 mmol), K_2CO_3 (2 mmol), precatalyst **C1** (1 mol%), and a mixture of THF/H_2O (3:1, 20 mL) were added to a 100 mL round-bottom flask. The reaction was stirred at room temperature for 12 hours. Upon completion, the reaction mixture was extracted, and the crude product was recrystallized from n-hexane to afford **3-mer** in a yellow-green solid. The intermediate was obtained in 90% yield without the need for column chromatography. ^{1}H NMR (400 MHz, $CDCl_3$) δ 7.89 (d, *J* = 8.3 Hz, 2H), 7.50 (d, *J* = 1.6 Hz, 2H), 7.34 (dd, *J* = 8.2, 1.6 Hz, 2H), 4.07 (dd, *J* = 7.6, 5.7 Hz, 2H), 1.57 (s, 2H), 1.29 – 1.23 (m, 7H), 0.94 – 0.87 (m, 6H). ^{13}C NMR (101 MHz, $CDCl_3$) δ 152.1, 148.0, 140.7, 137.2, 135.9, 135.7, 126.1, 124.2, 121.4, 120.7, 55.5, 40.2, 31.7, 29.9, 29.1, 23.8, 22.6, 14.0. HRMS (ESI$^+$): 613.3118 (calcd for $C_{39}H_{47}Cl_2N_2$, $[M+H]^+$ 613.3116).

3. NMR spectra for the products

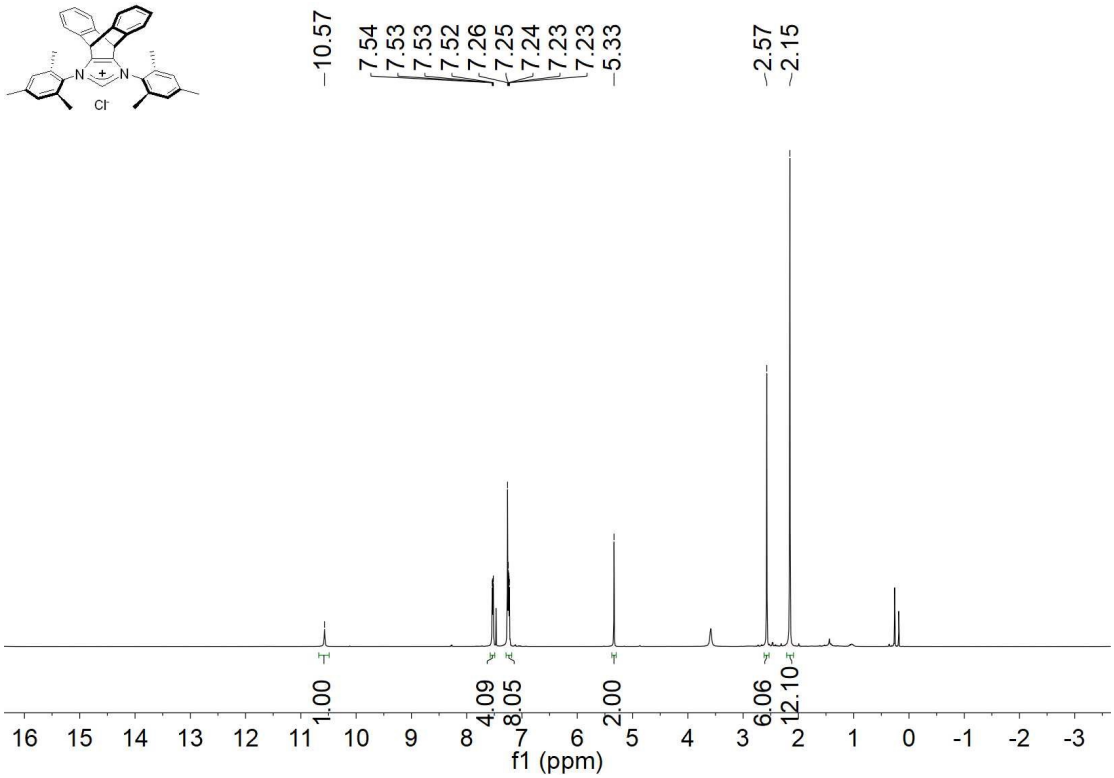

Figure S1. The ^{1}H NMR spectrums of **L1**

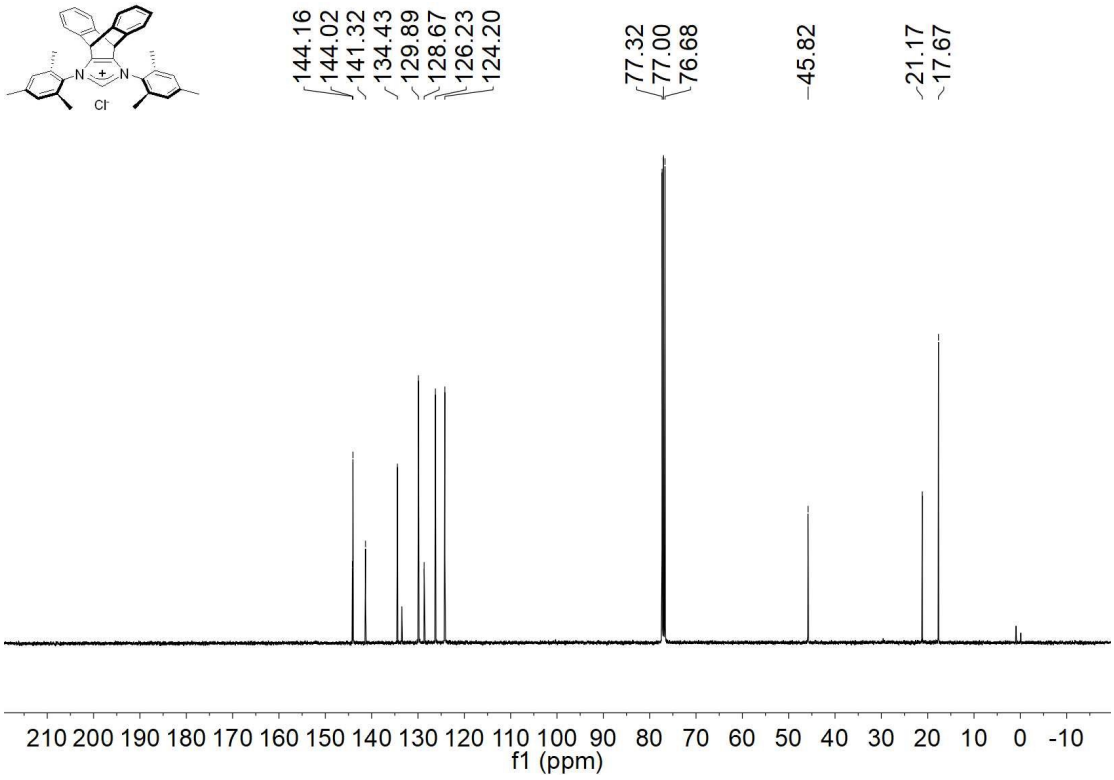

Figure S2. The ^{13}C NMR spectrums of **L1**

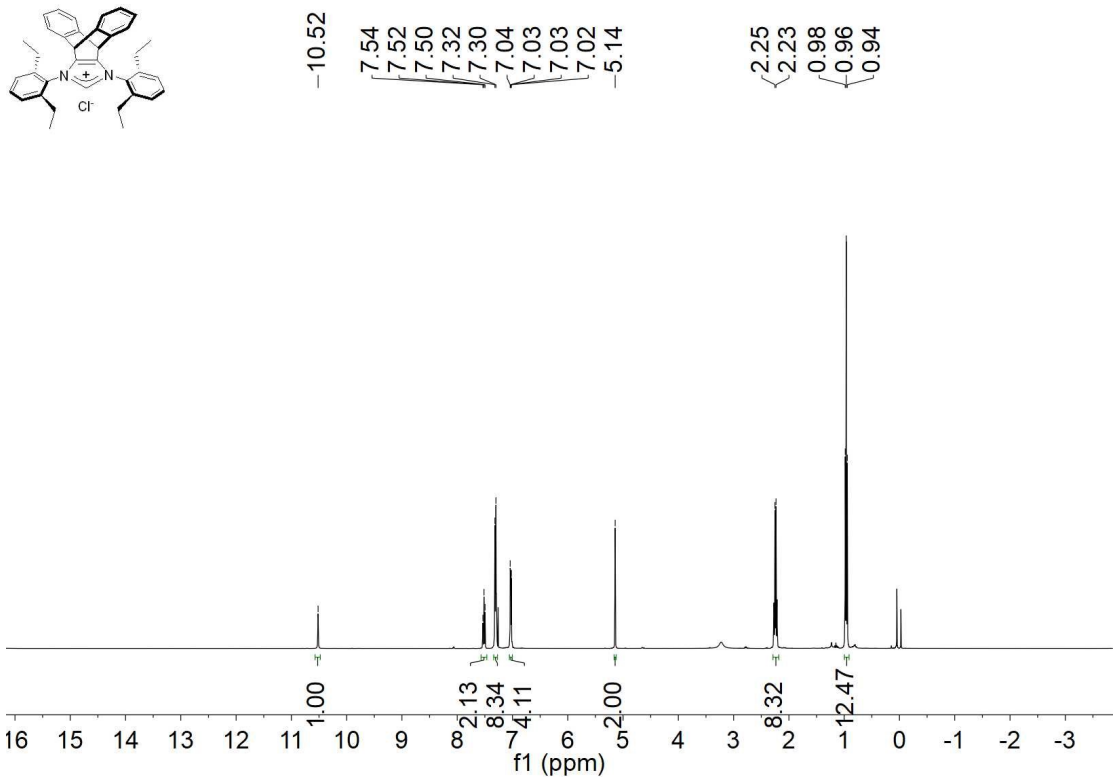

Figure S3. The ^{1}H NMR spectrums of **L2**

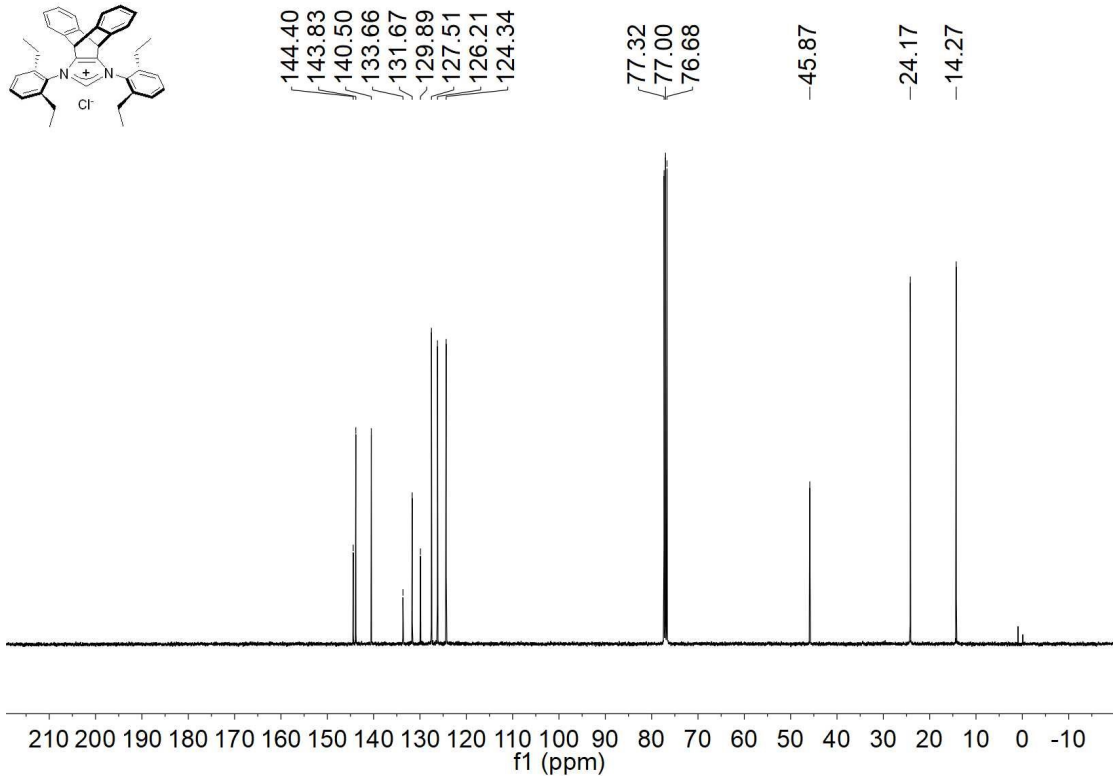

Figure S4. The ^{13}C NMR spectrums of **L2**

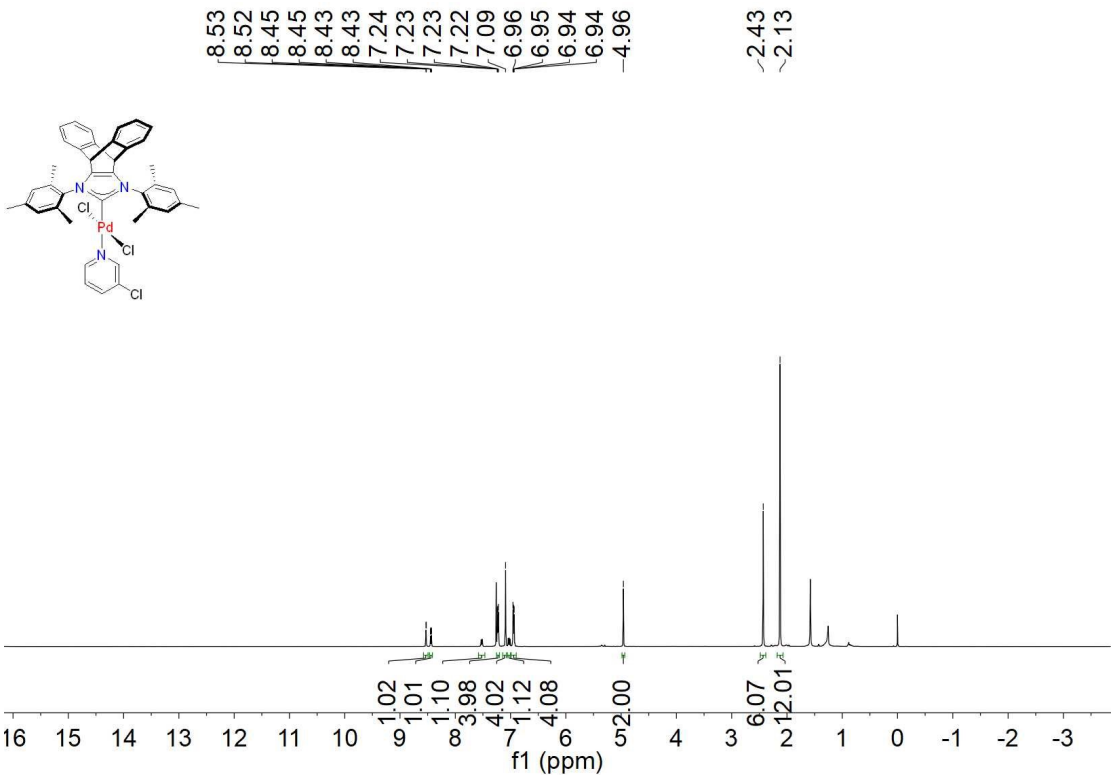

Figure S5. The ^{1}H NMR spectrums of **C1**

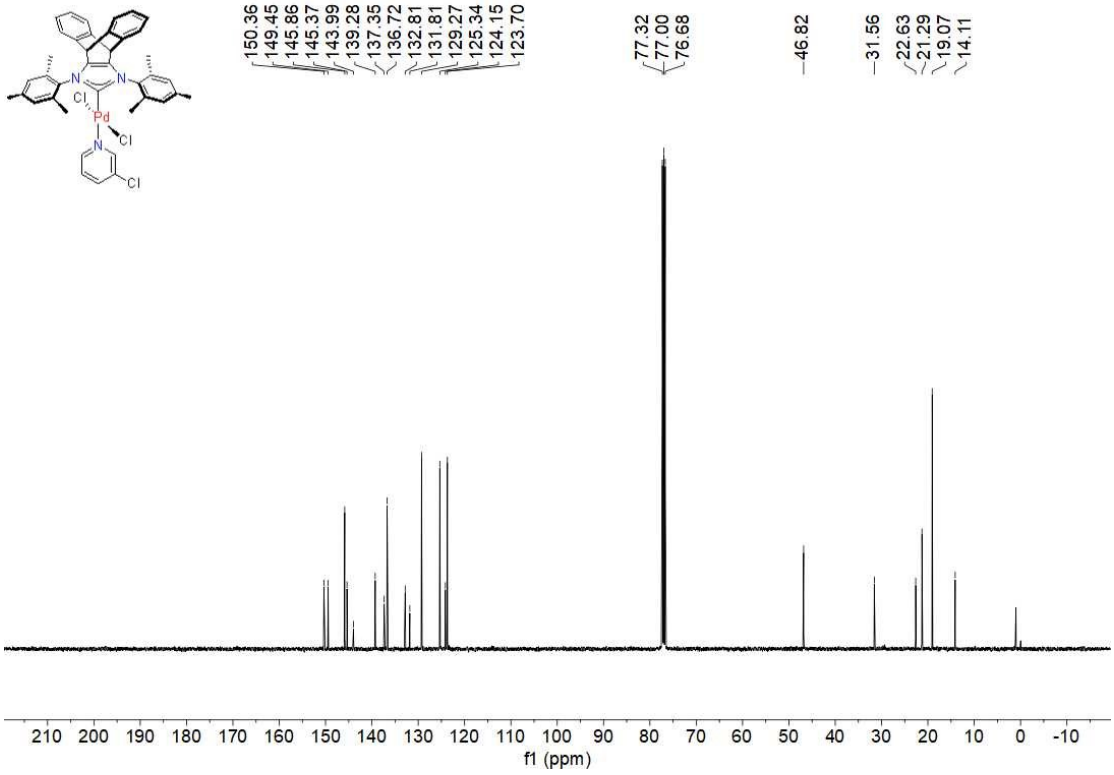

Figure S6. The ^{13}C NMR spectrums of **C1**

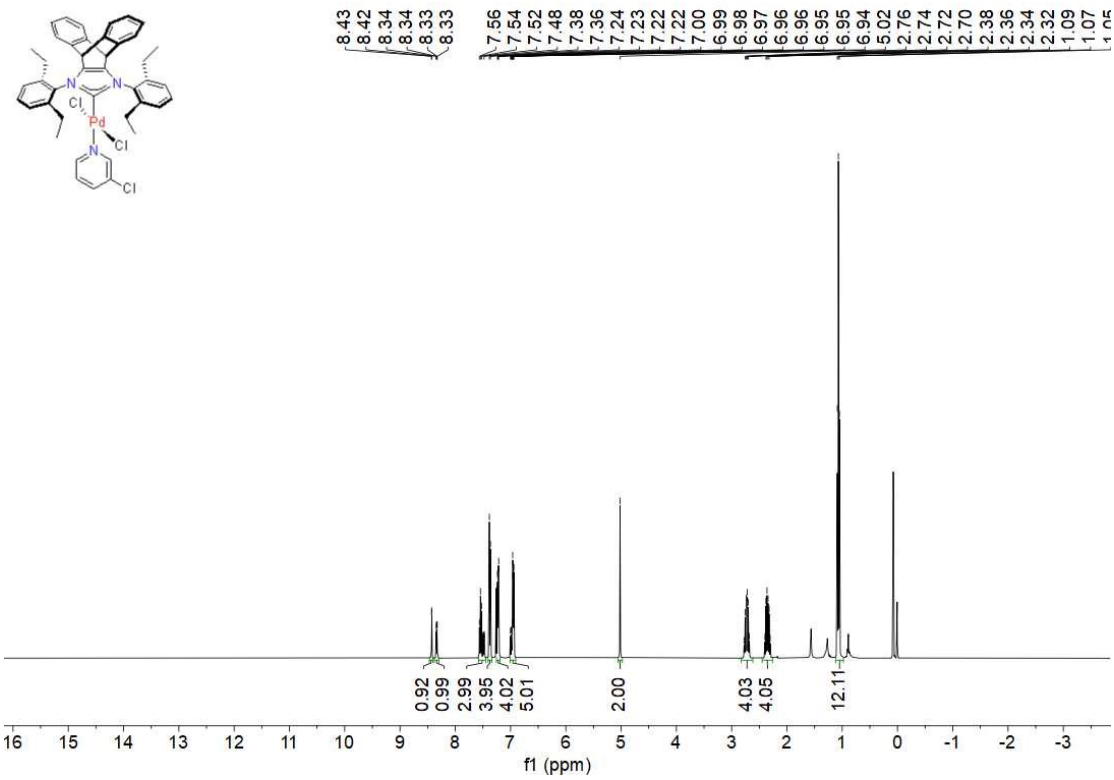

Figure S7. The ^{1}H NMR spectrums of **C2**

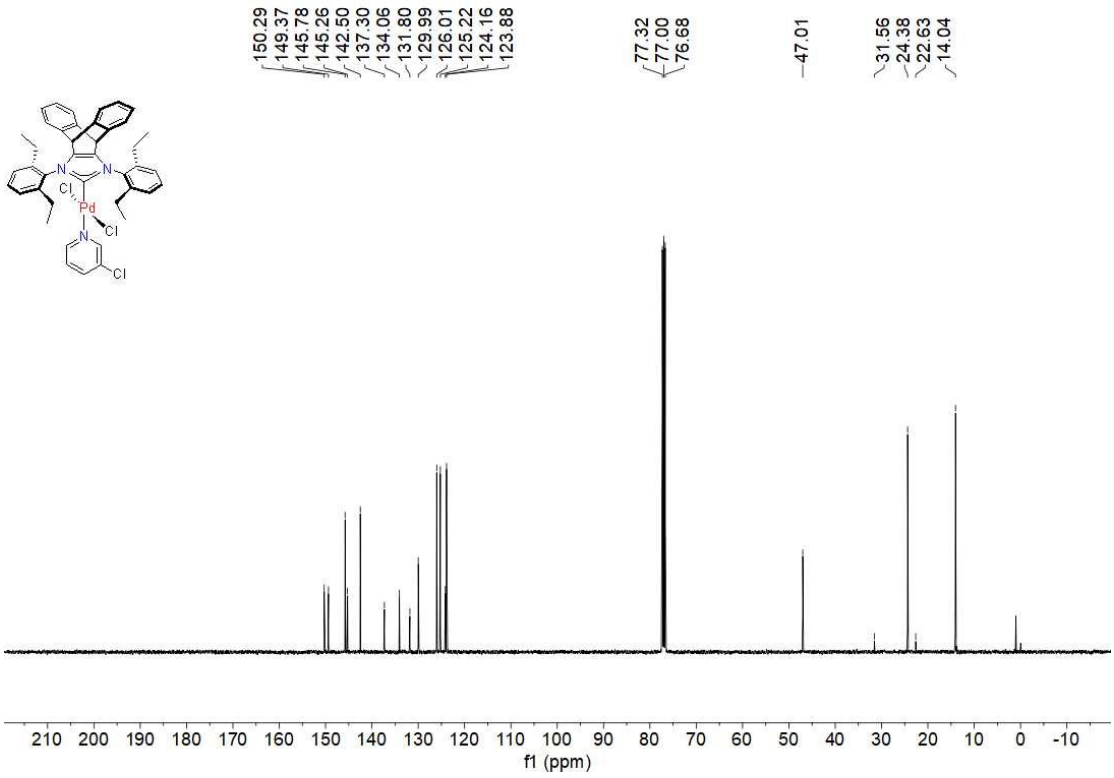

Figure S8. The ^{13}C NMR spectrums of **C2**

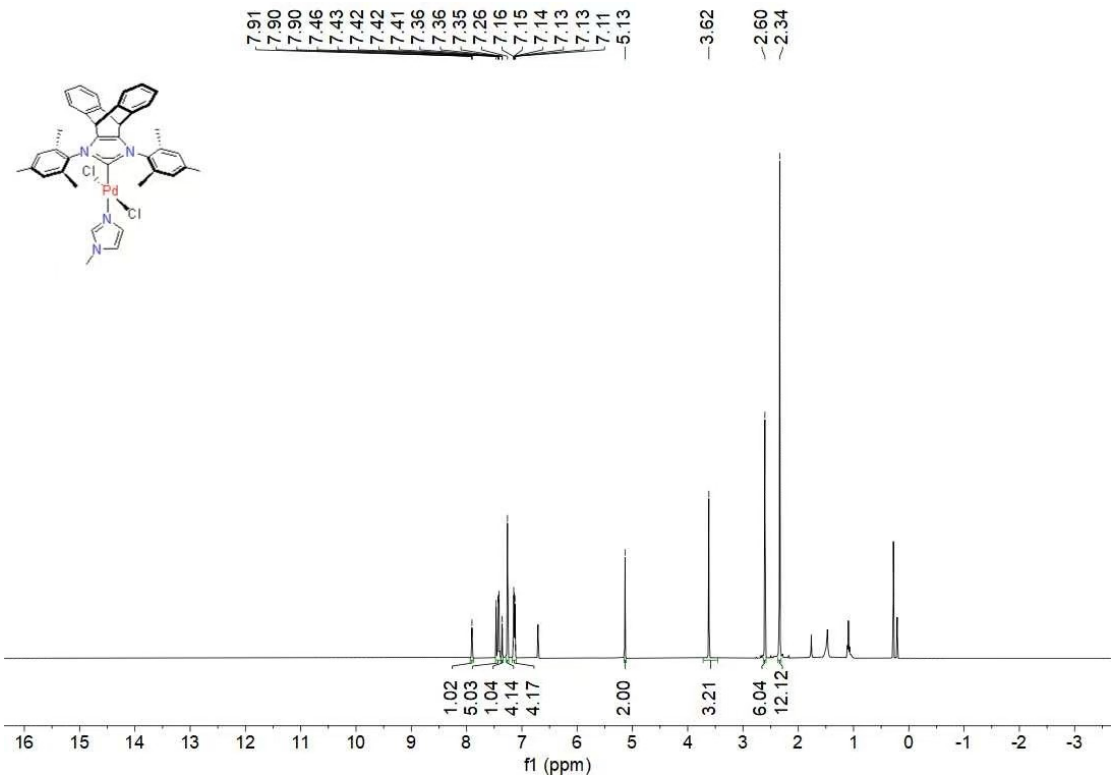

Figure S9. The ^{1}H NMR spectrums of **C3**

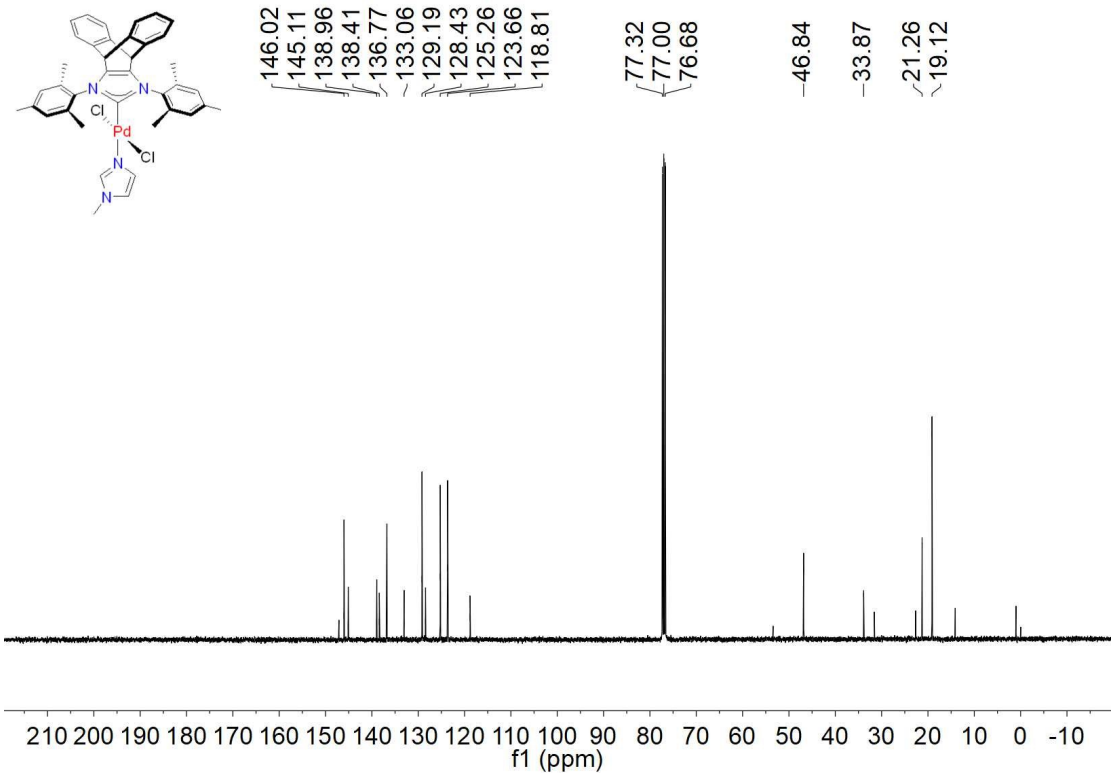

Figure S10. The ^{13}C NMR spectrums of **C3**

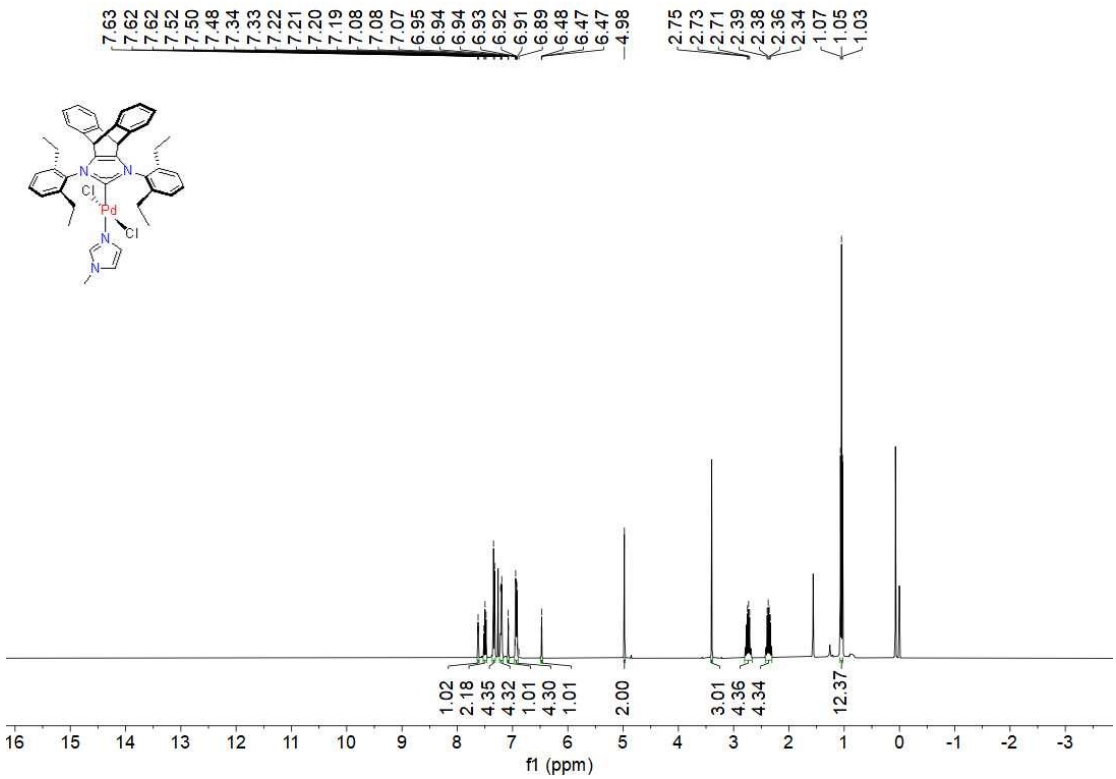

Figure S11. The ^{1}H NMR spectrums of **C4**

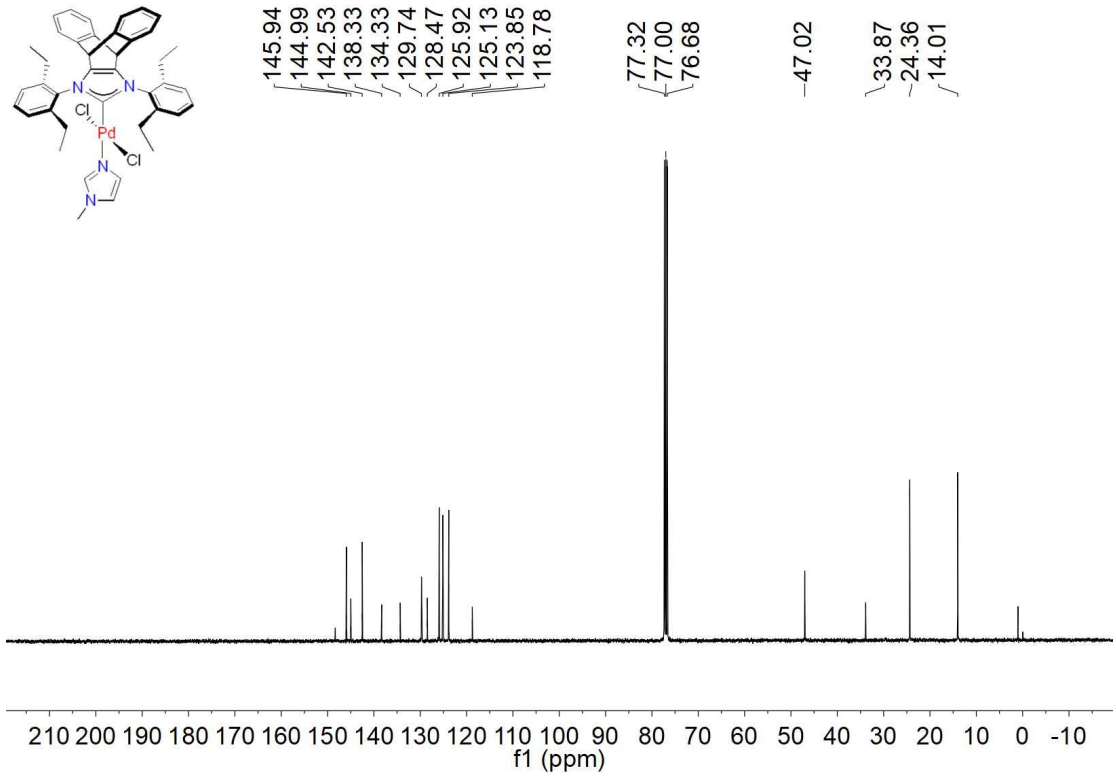

Figure S12. The ^{13}C NMR spectrums of **C4**

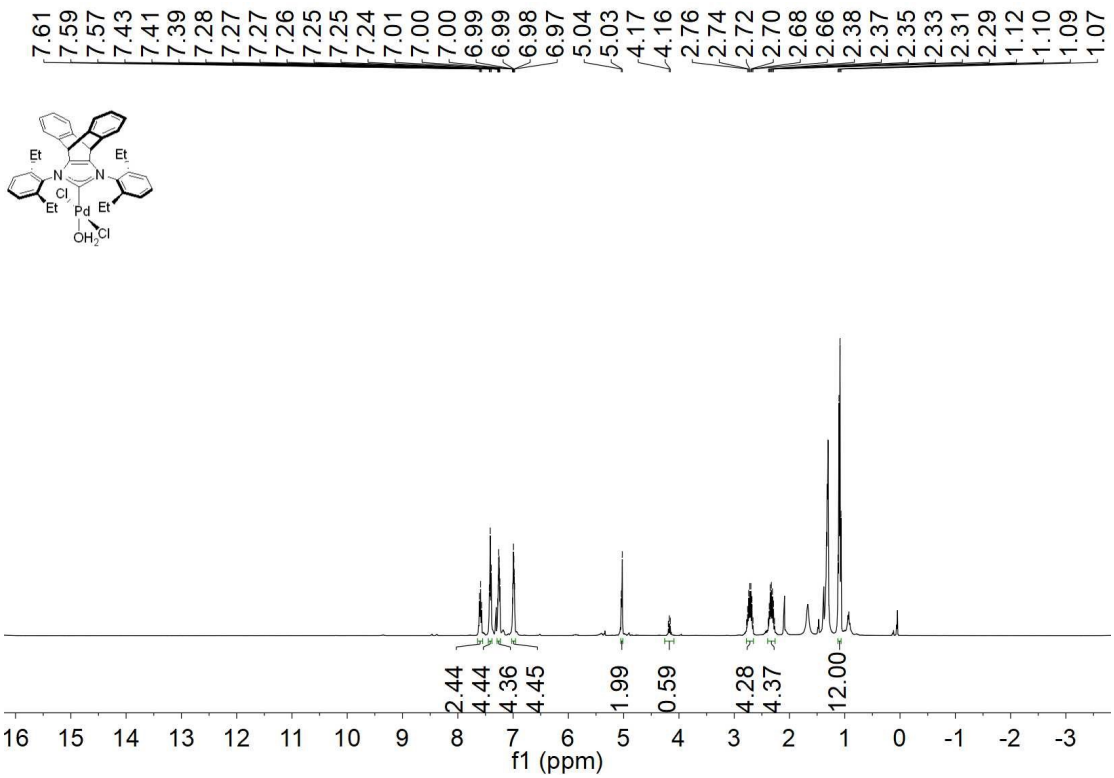

Figure S13. The ^{1}H NMR spectrums of **C5**

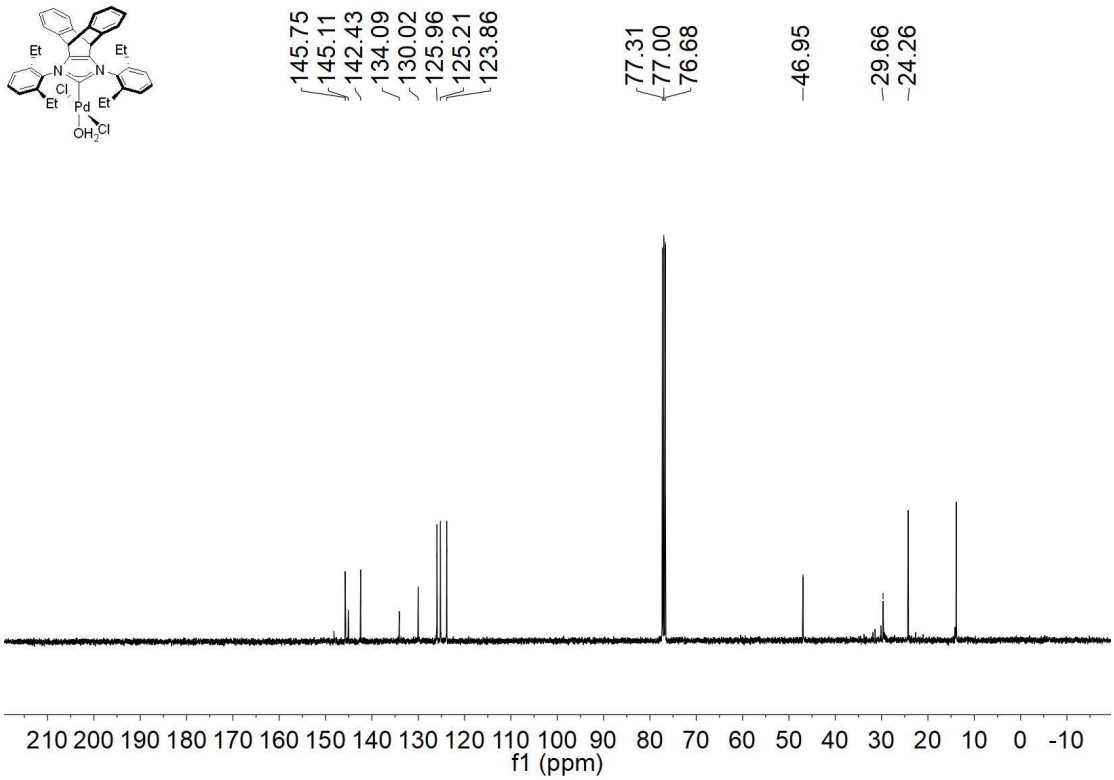

Figure S14. The ^{13}C NMR spectrums of **C5**

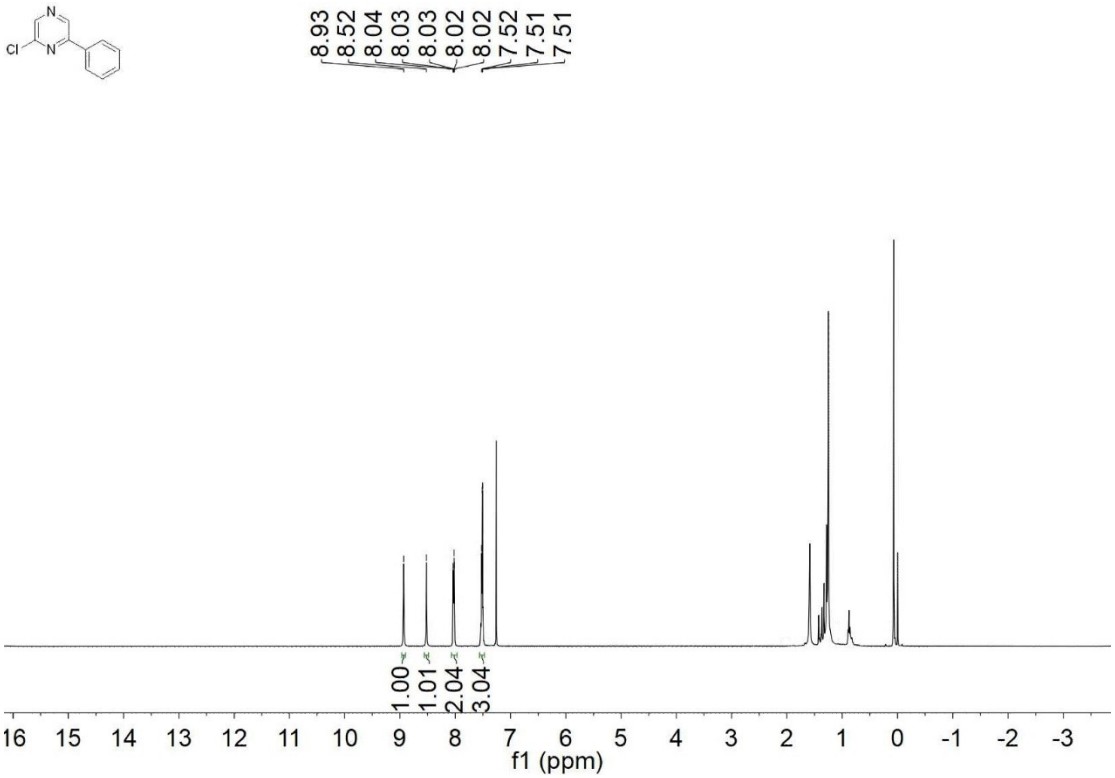

Figure S15. The ^{1}H NMR spectrums of **A**

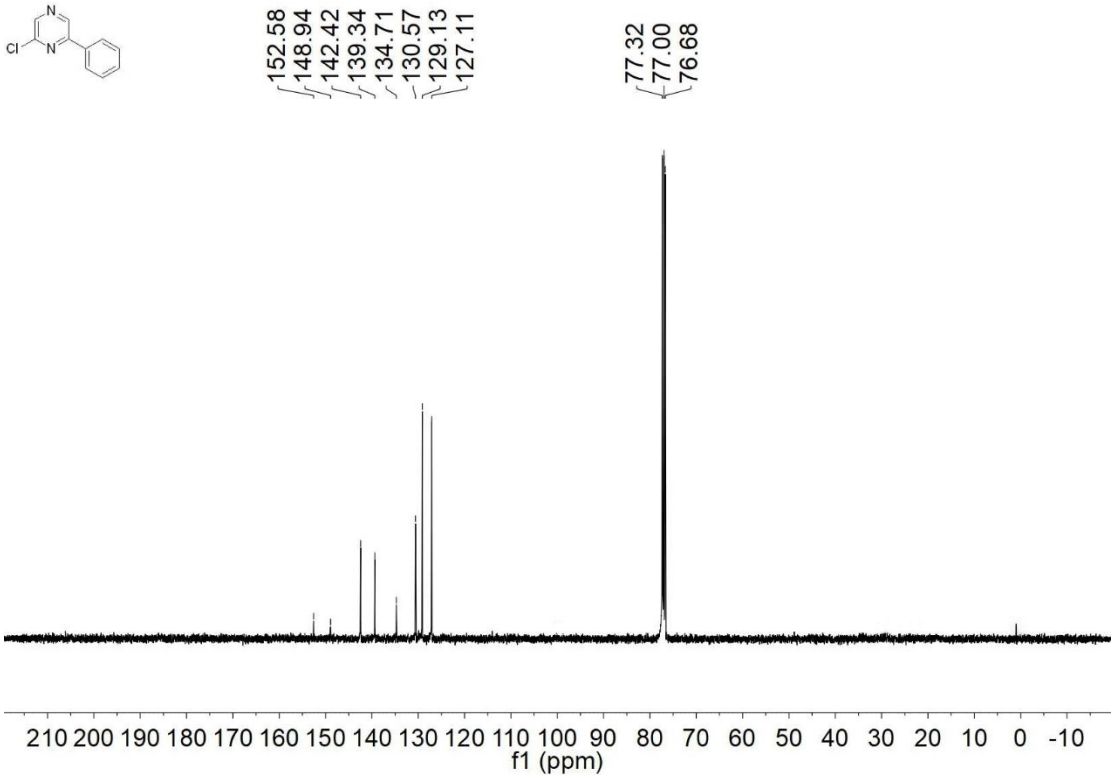

Figure S16. The ^{13}C NMR spectrums of **A**

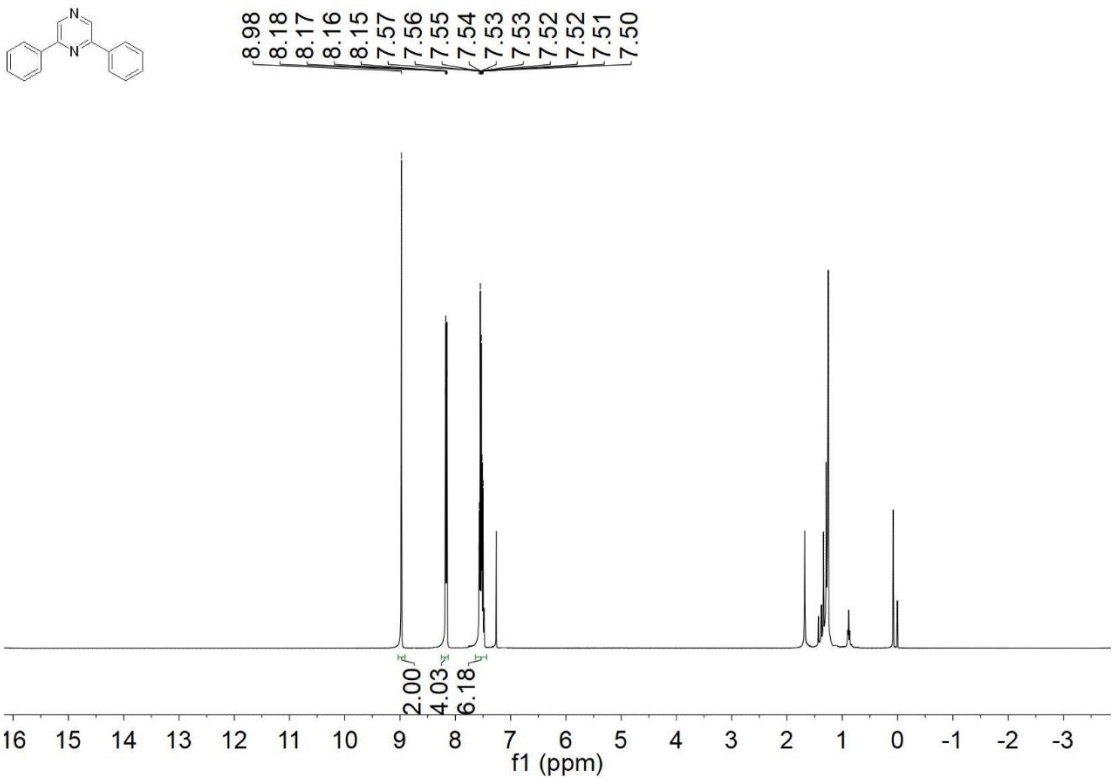

Figure S17. The ^{1}H NMR spectrums of **B**

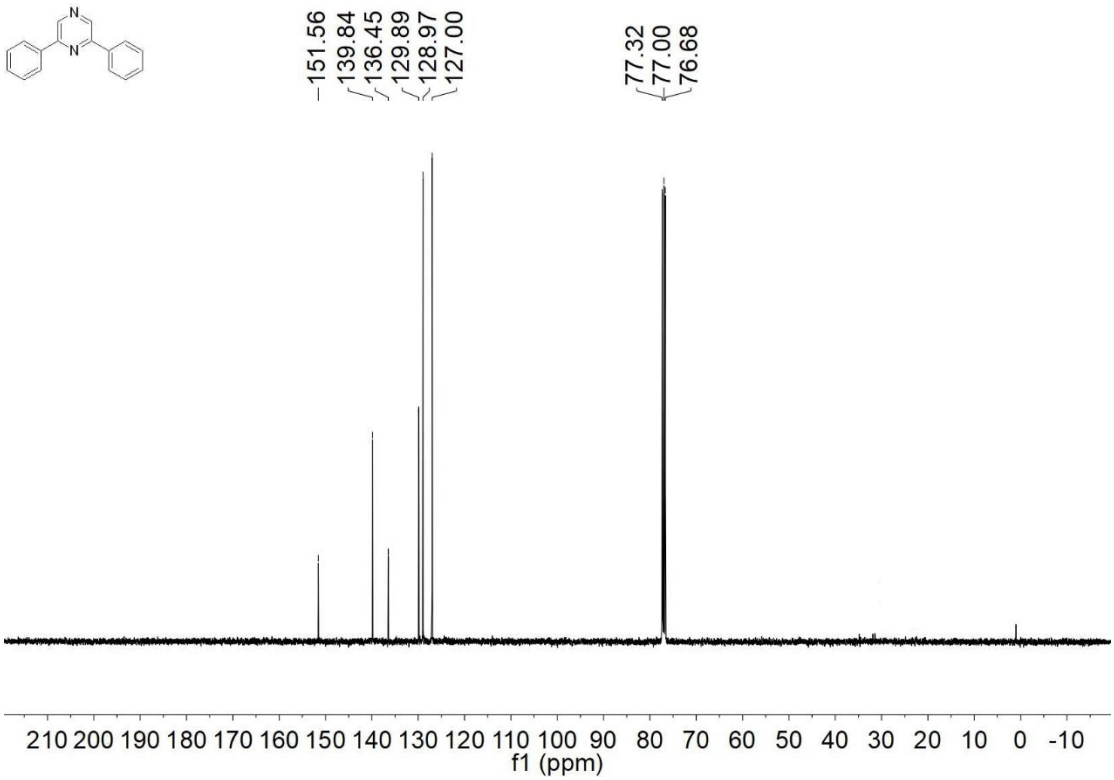

Figure S18. The ^{13}C NMR spectrums of **B**

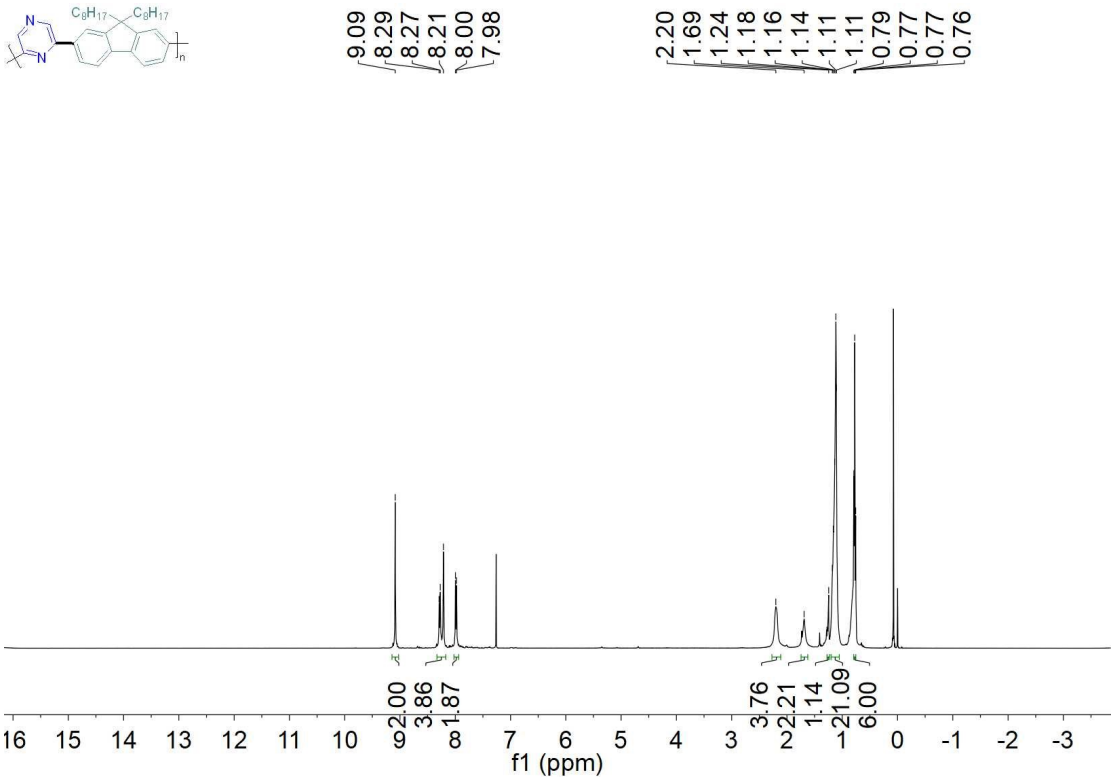

Figure S19. The NMR spectrums of **P1**.

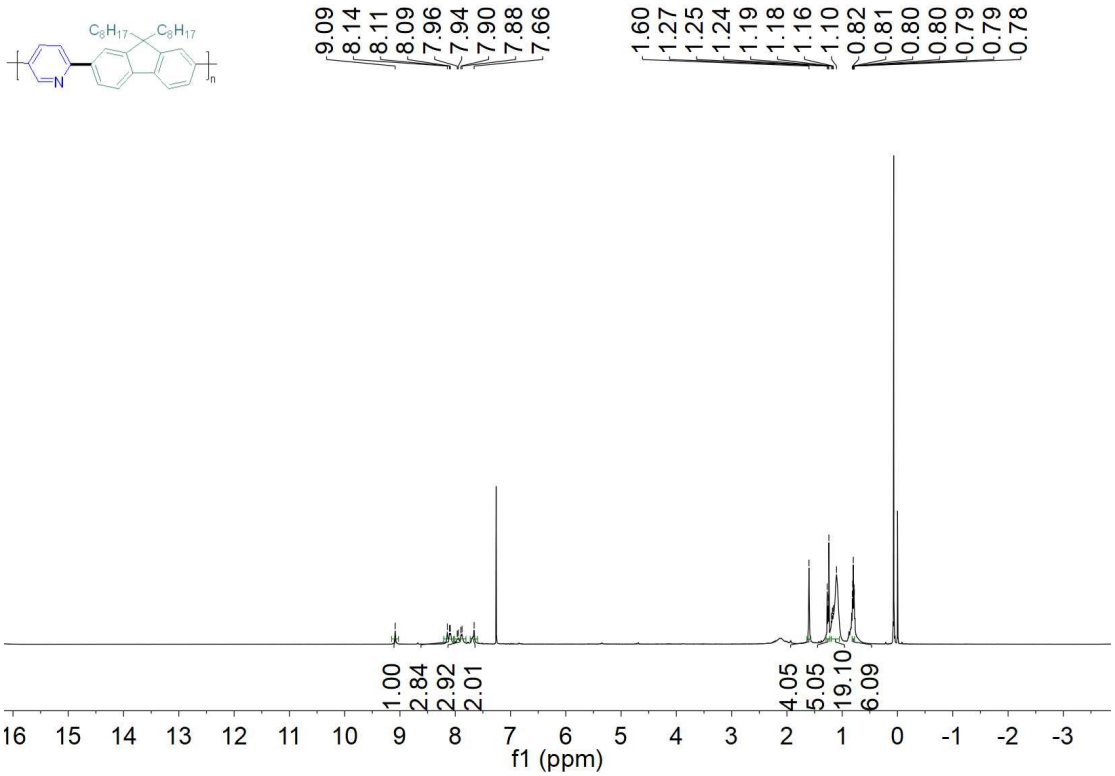

Figure S20. The NMR spectrums of **P2**.

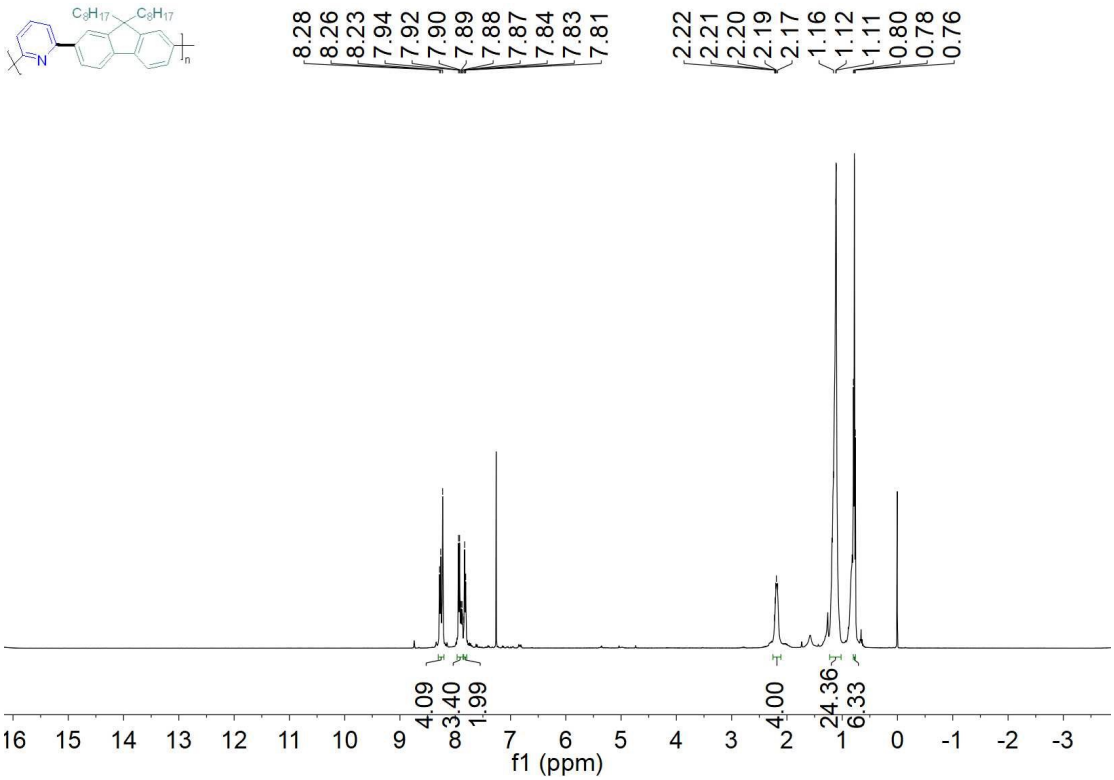

Figure S21. The NMR spectrums of **P3**.

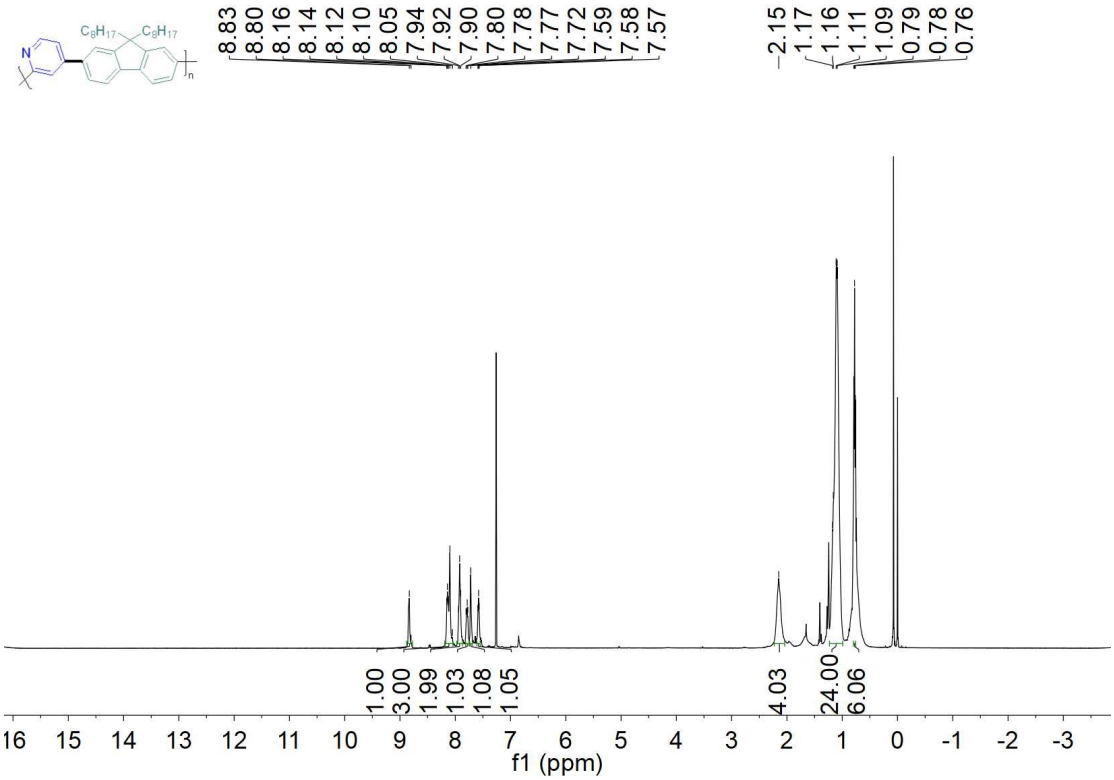

Figure S22. The NMR spectrums of **P4**.

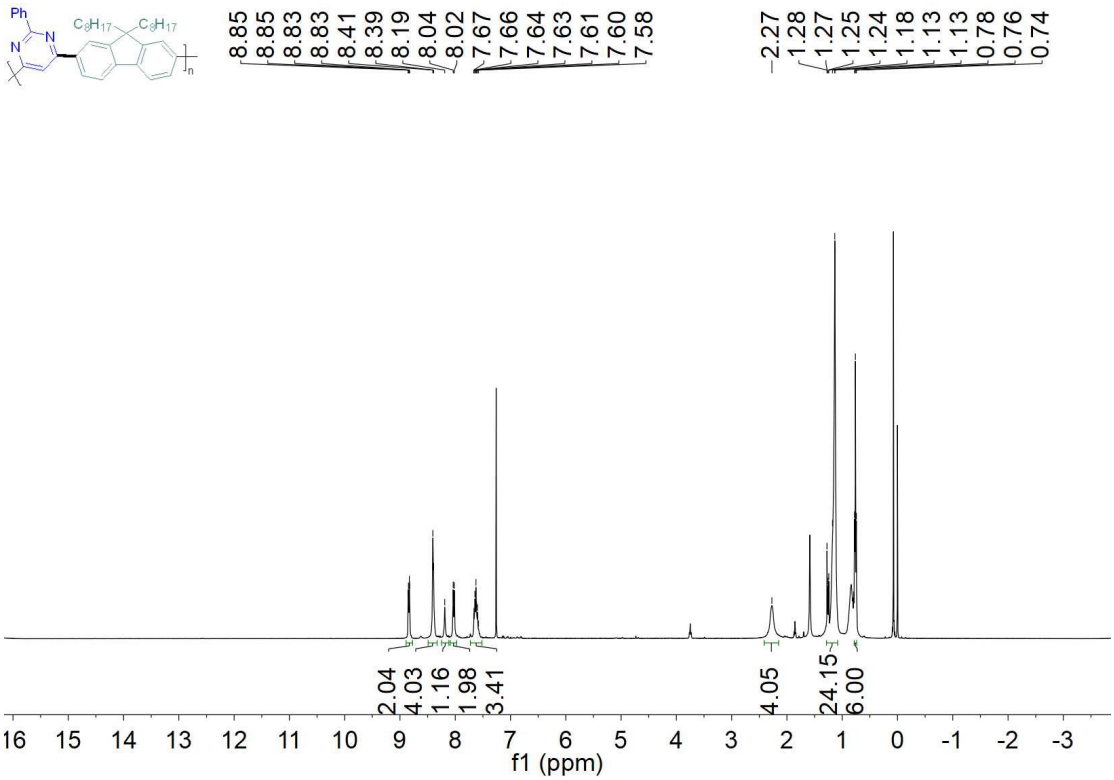

Figure S23. The NMR spectrums of **P5**.

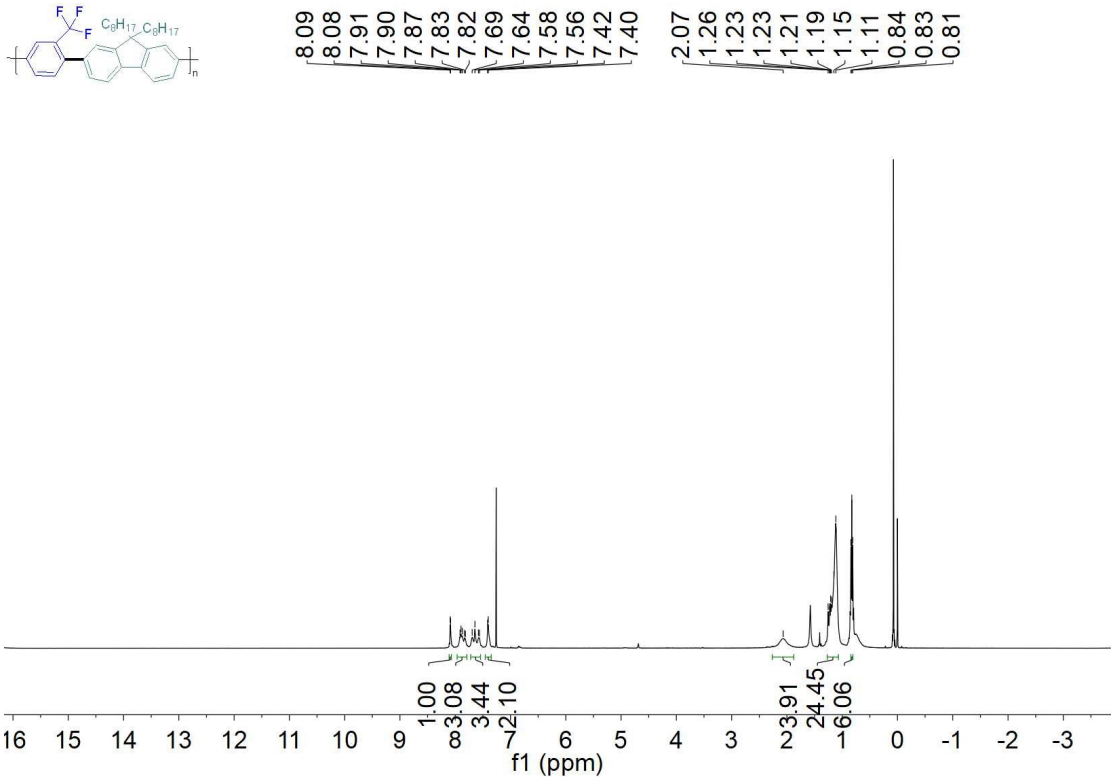

Figure S24. The NMR spectrums of **P6**.

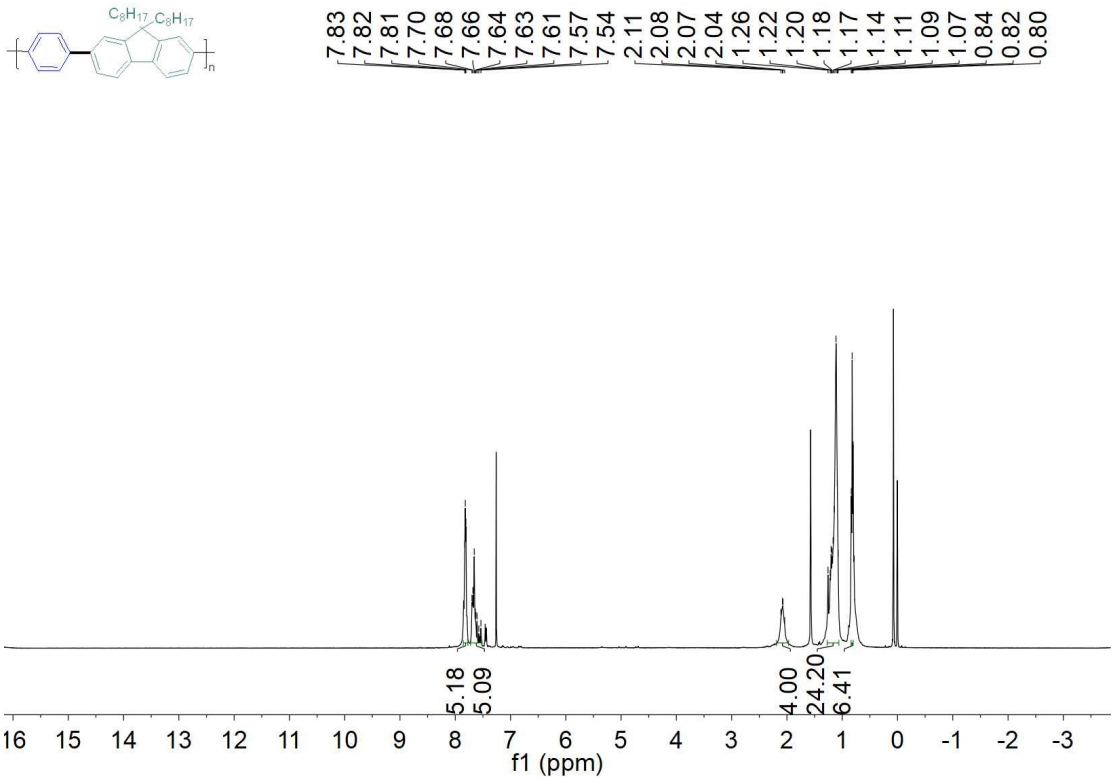

Figure S25. The NMR spectrums of **P7**.

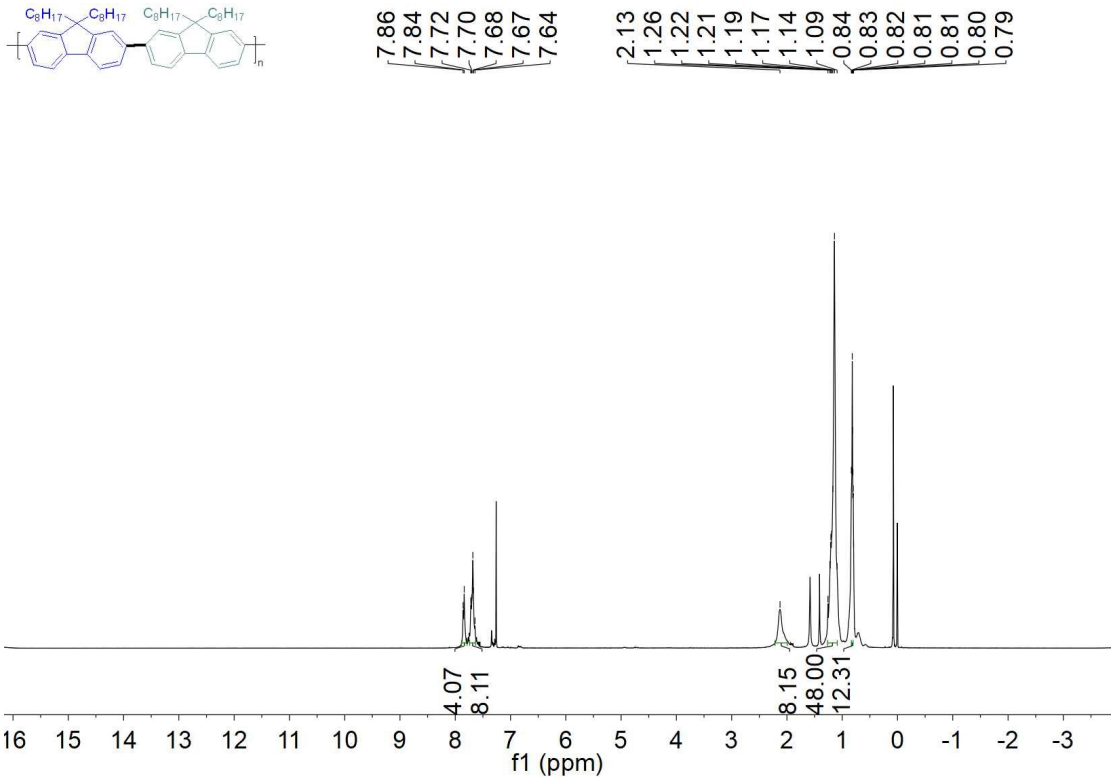

Figure S26. The NMR spectrums of **P8**.

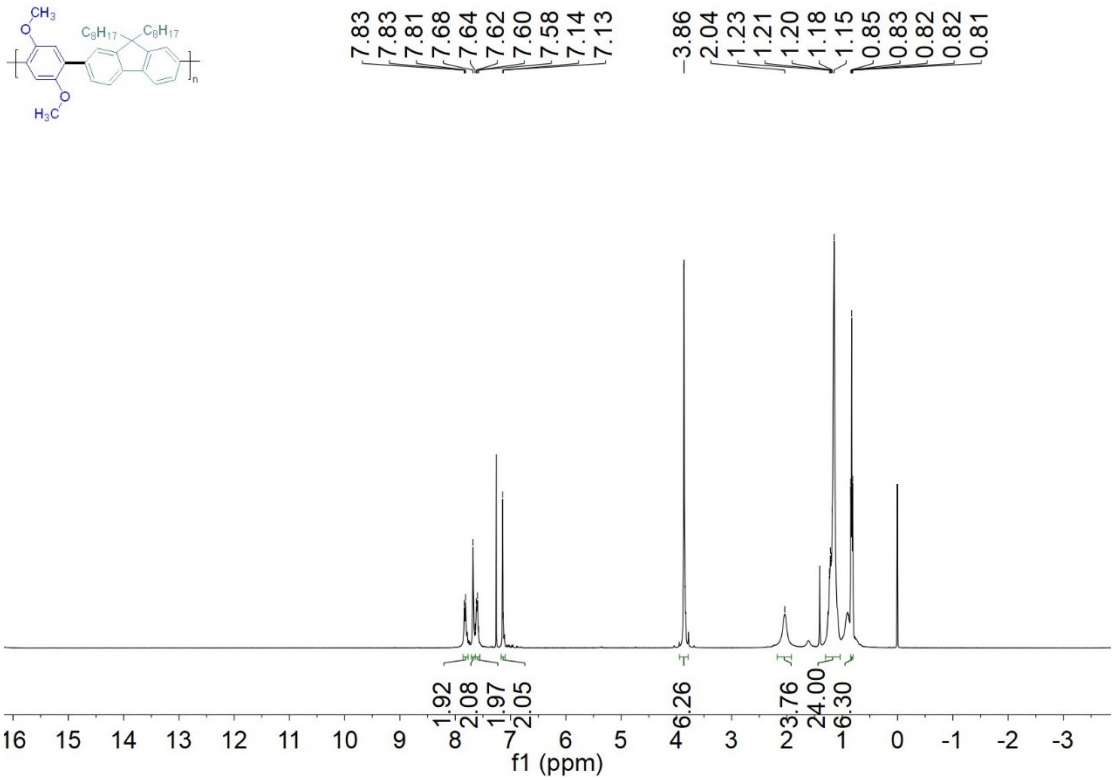

Figure S27. The NMR spectrums of **P9**.

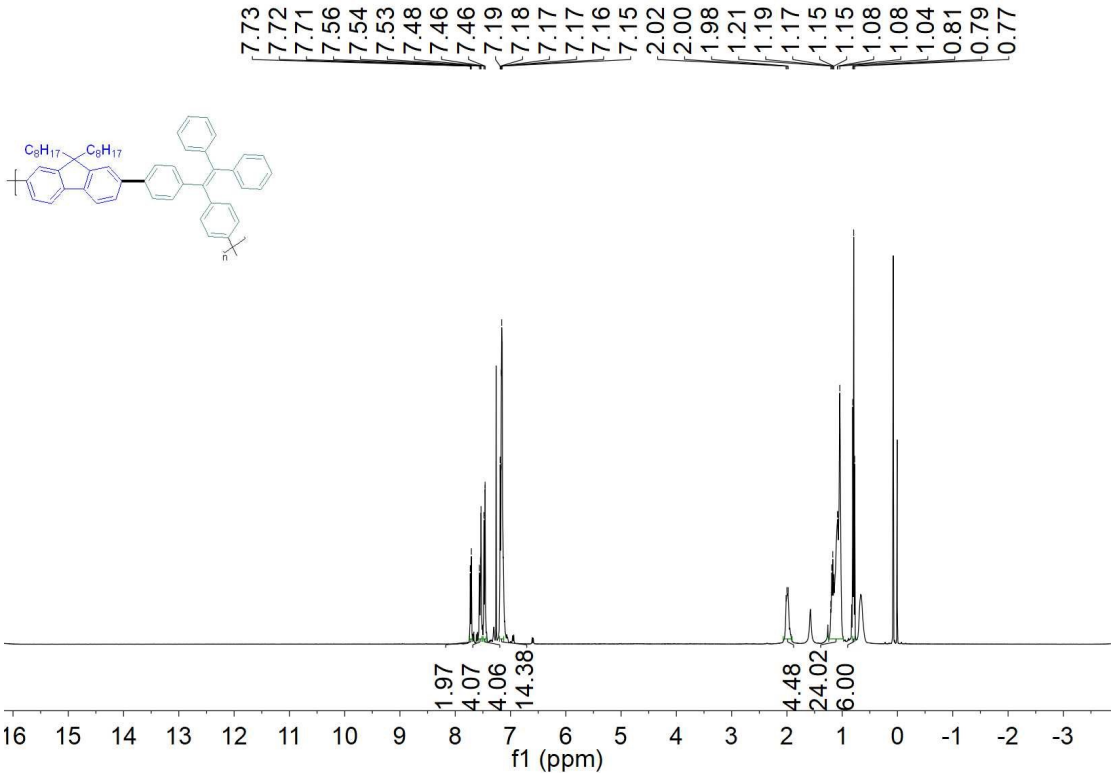

Figure S28. The ^{1}H NMR spectrum of **P11.**

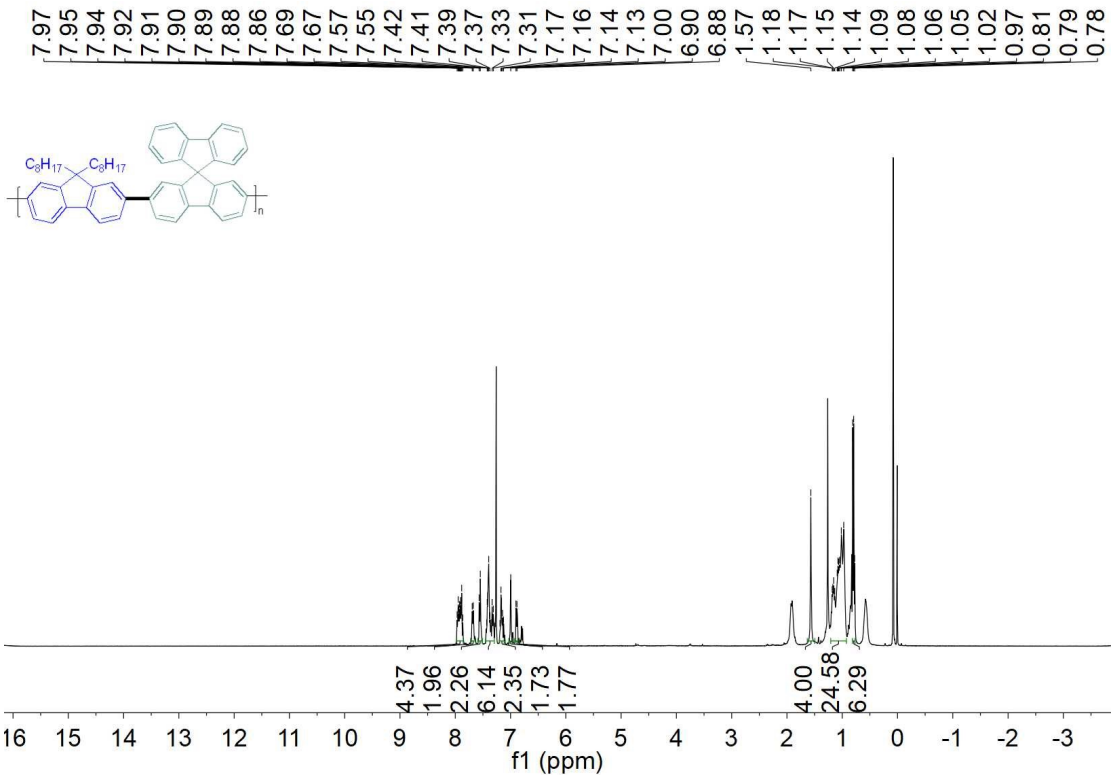

Figure S29. The ^{1}H NMR spectrum of **P12.**

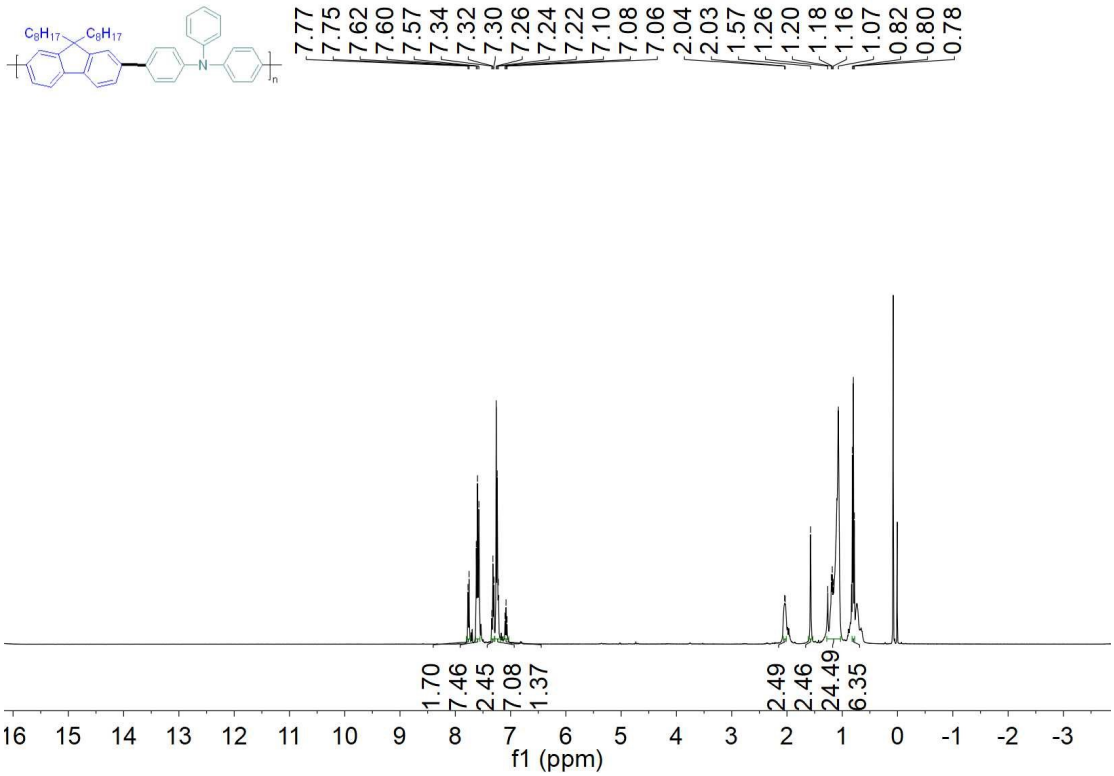

Figure S30. The ^{1}H NMR spectrum of **P13.**

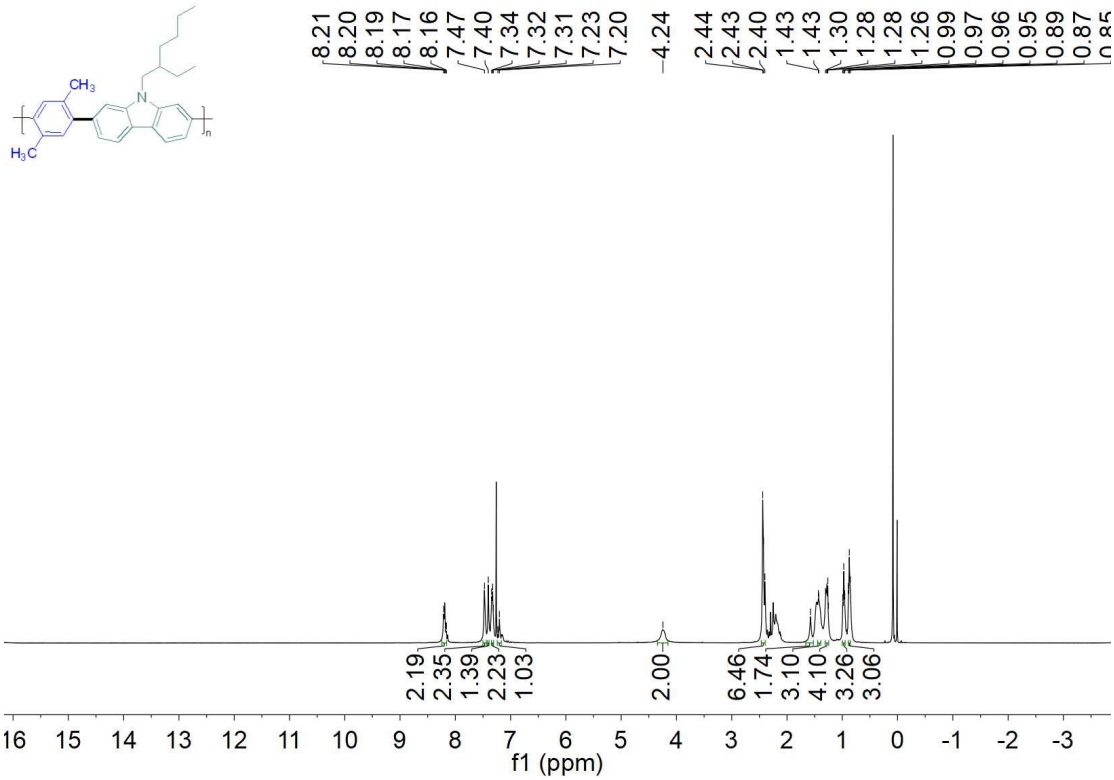

Figure S31. The ^{1}H NMR spectrum of **P14.**

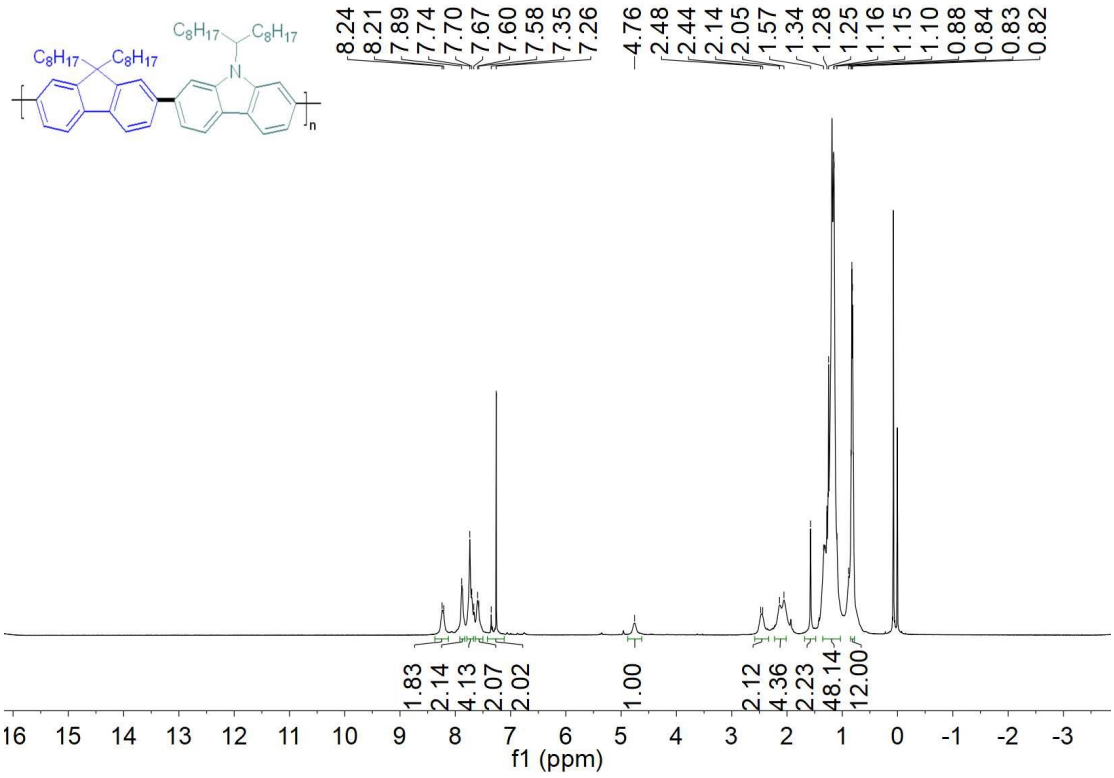

Figure S32. The ^{1}H NMR spectrum of **P15.**

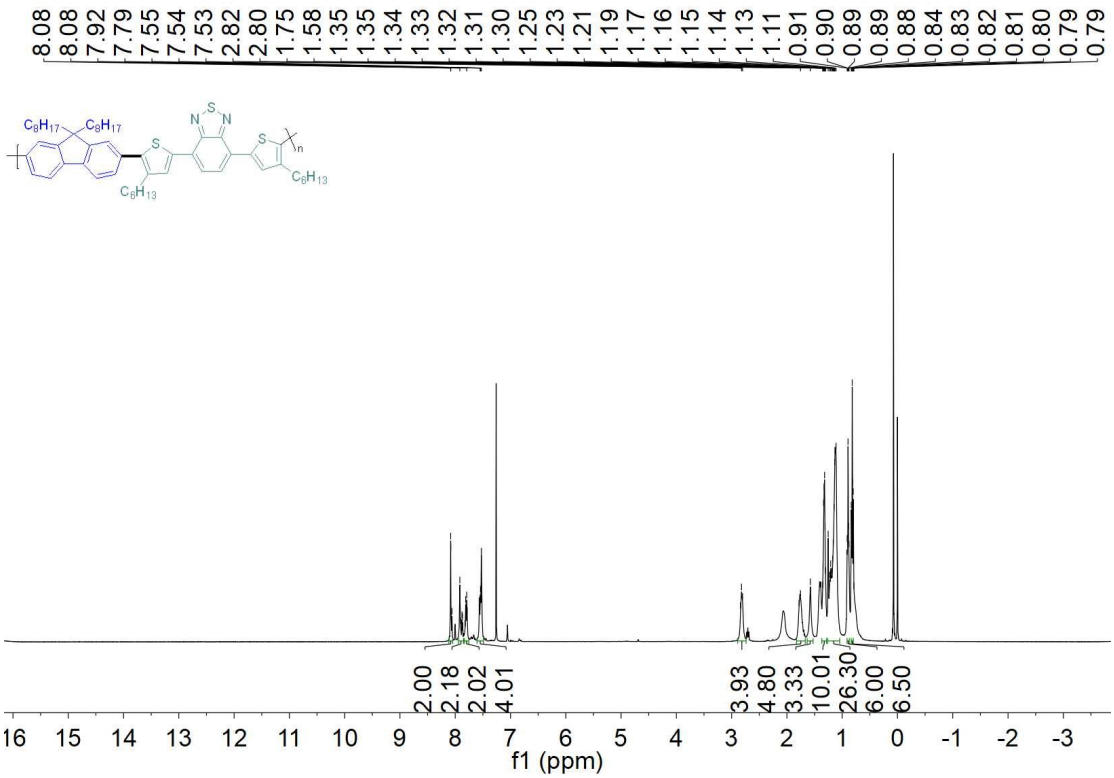

Figure S33. The ^{1}H NMR spectrum of **P16.**

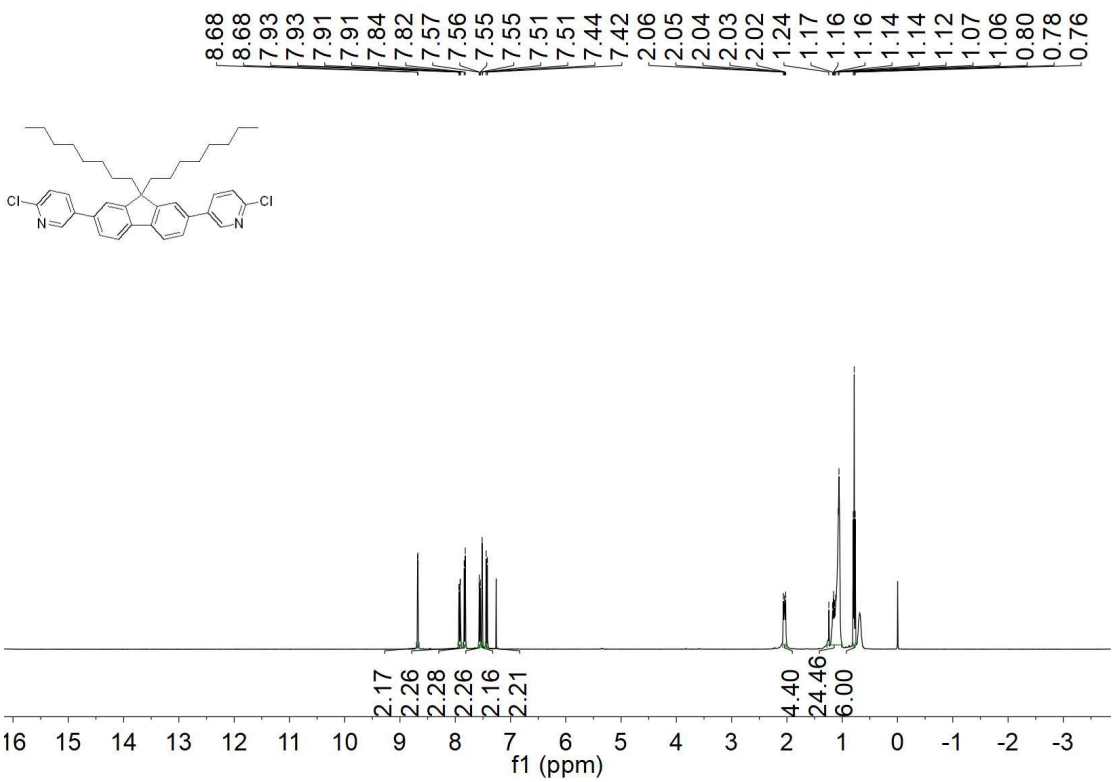

Figure S34. The ^{1}H NMR spectrums of **3-mer.**

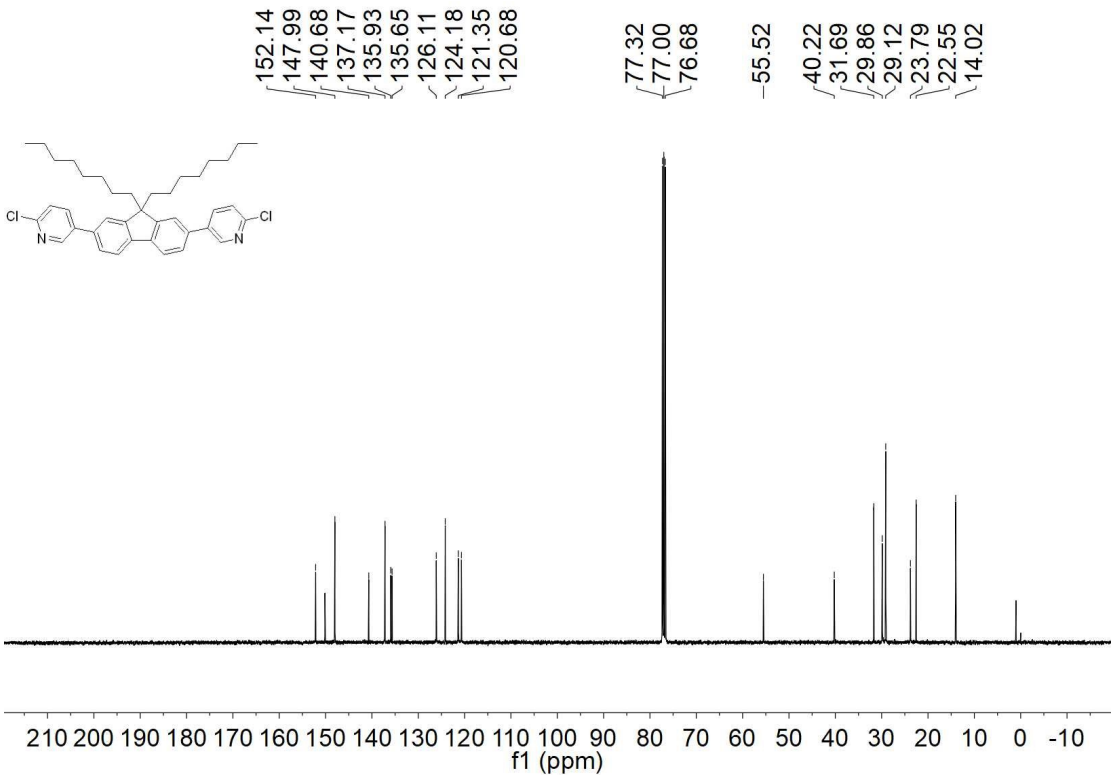

Figure S35. The ^{13}C NMR spectrums of **3-mer.**

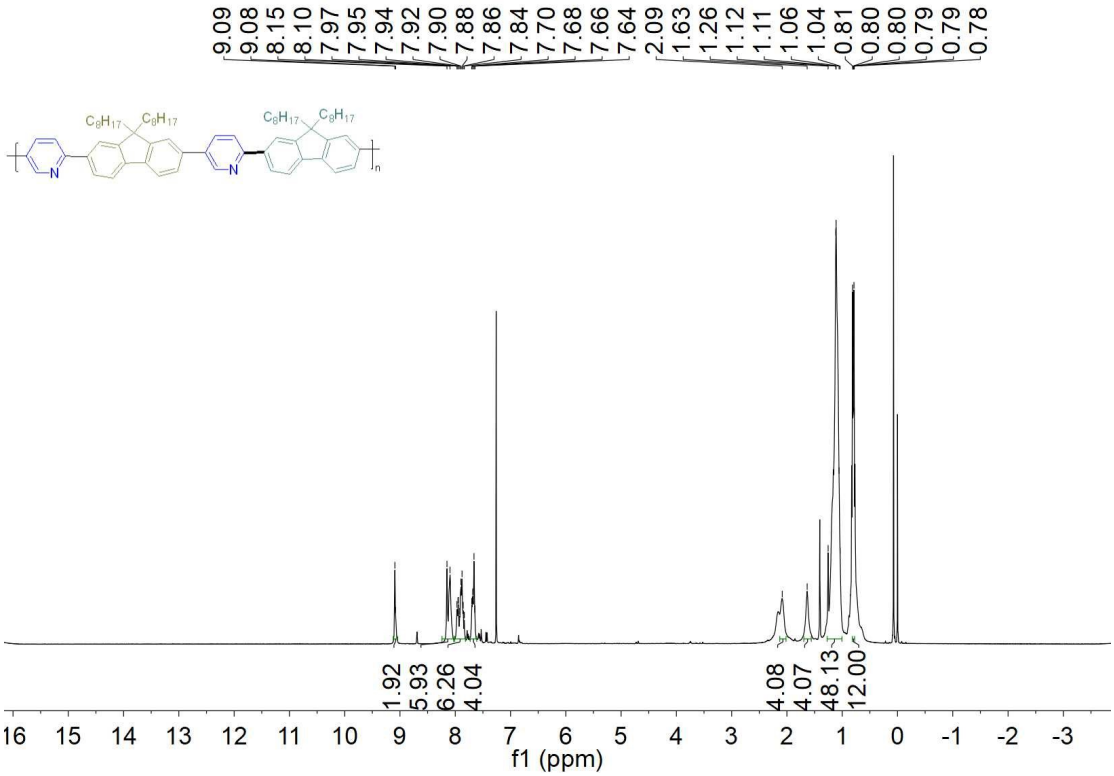

Figure S36. The ^{1}H NMR spectrum of **P17.**

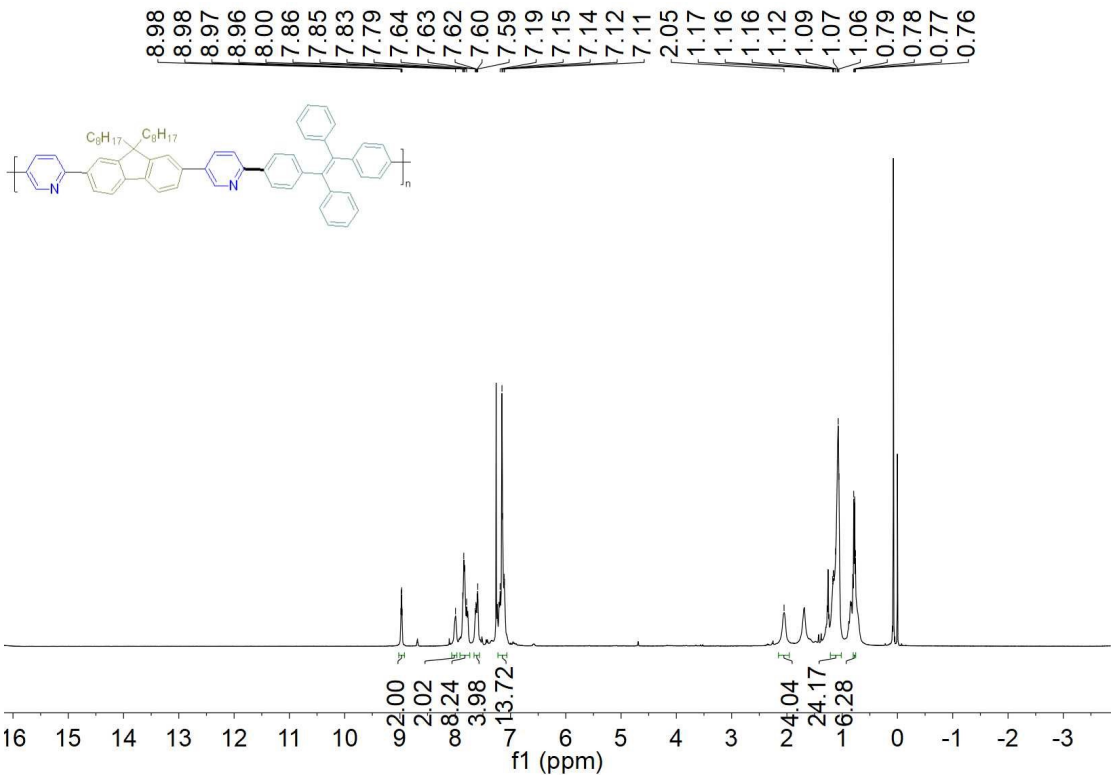

Figure S37. The ^{1}H NMR spectrum of **P18.**

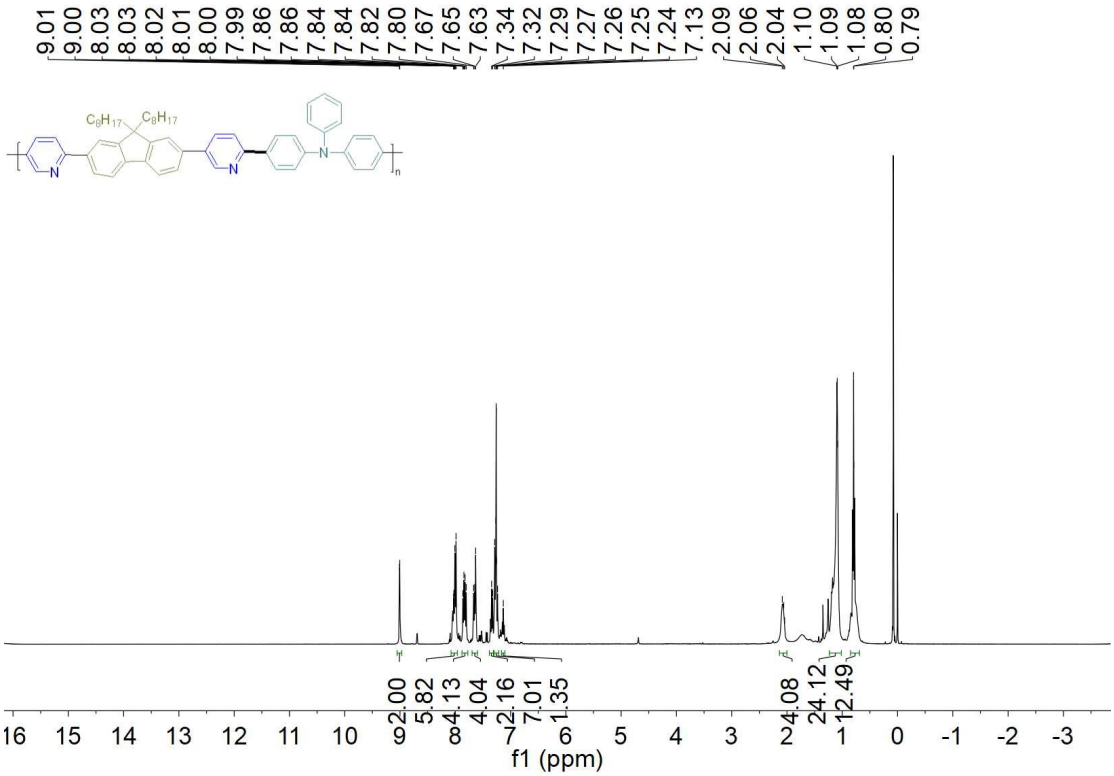

Figure S38. The ^{1}H NMR spectrum of **P19.**

4. The Optical Spectra: UV-Vis Absorption and Fluorescence Emission

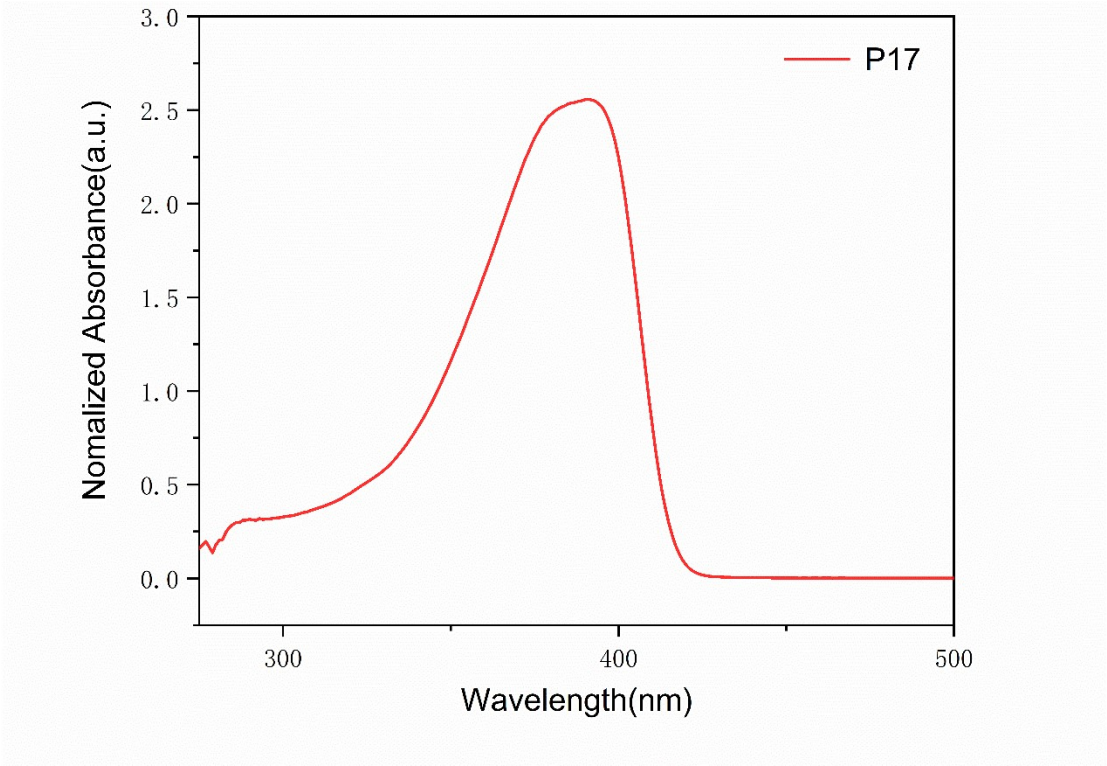

Figure S39. UV-Vis absorption spectrum of **P17.**

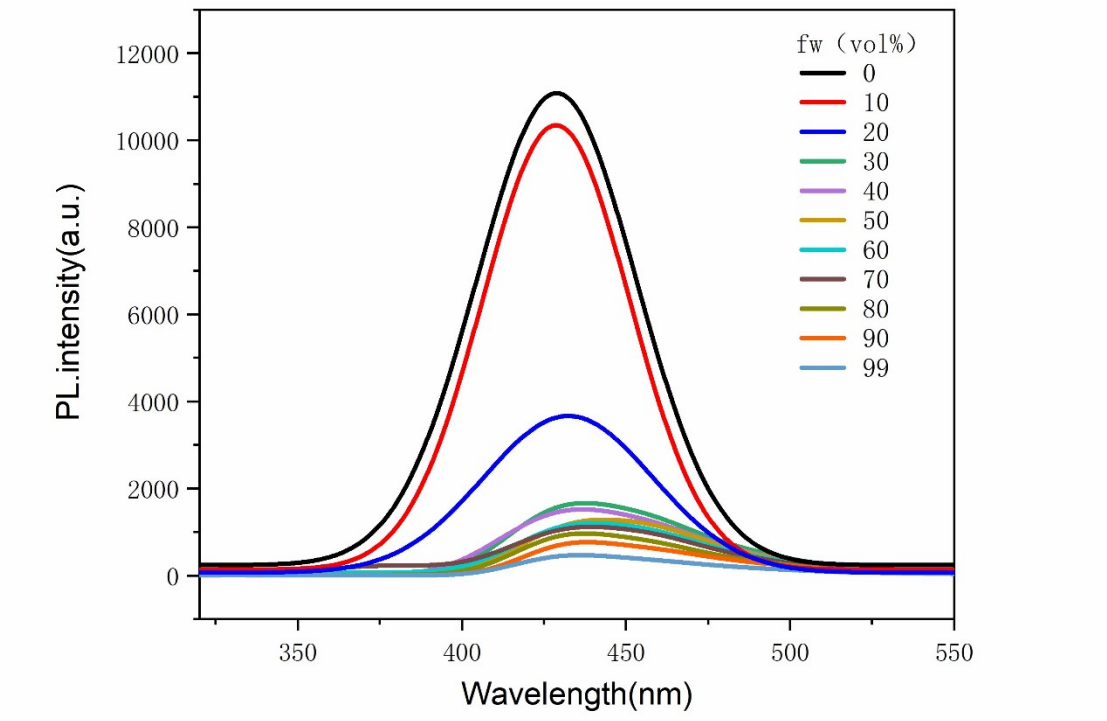

Figure S40. Fluorescence emission Spectrum of **P17.**

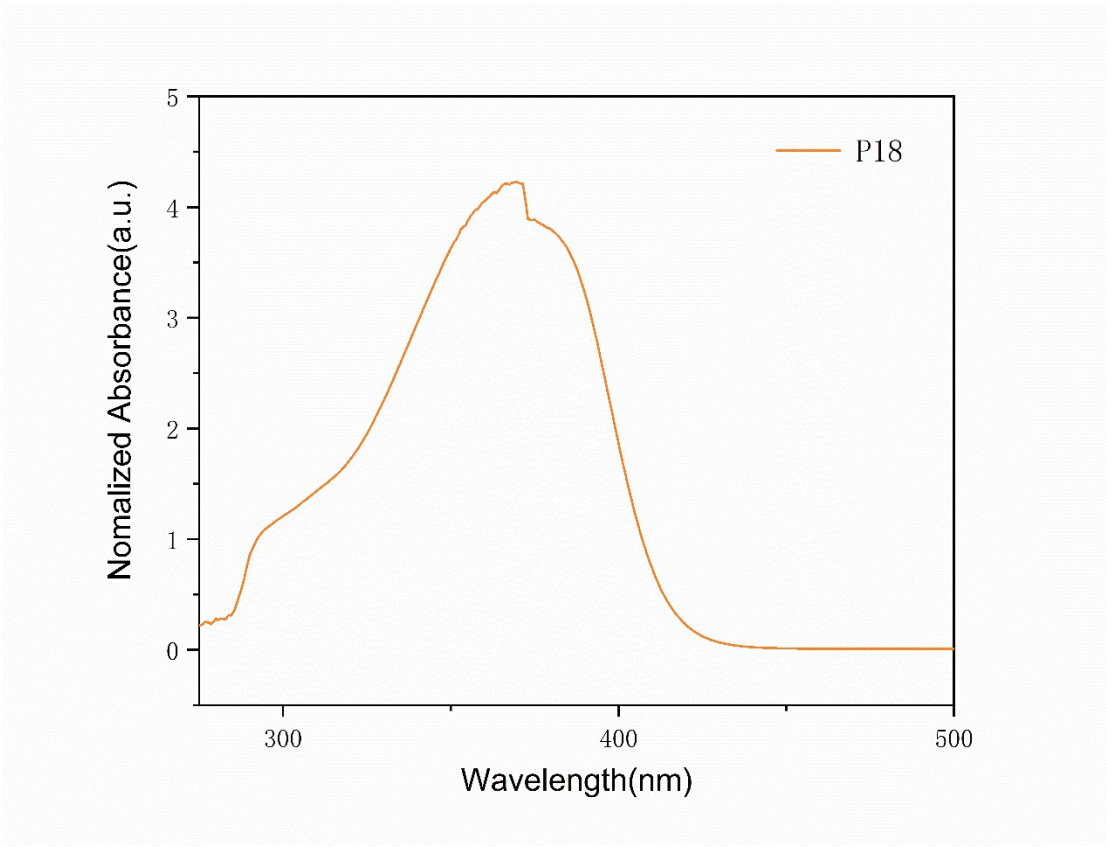

Figure S41. UV-Vis absorption spectrum of **P18.**

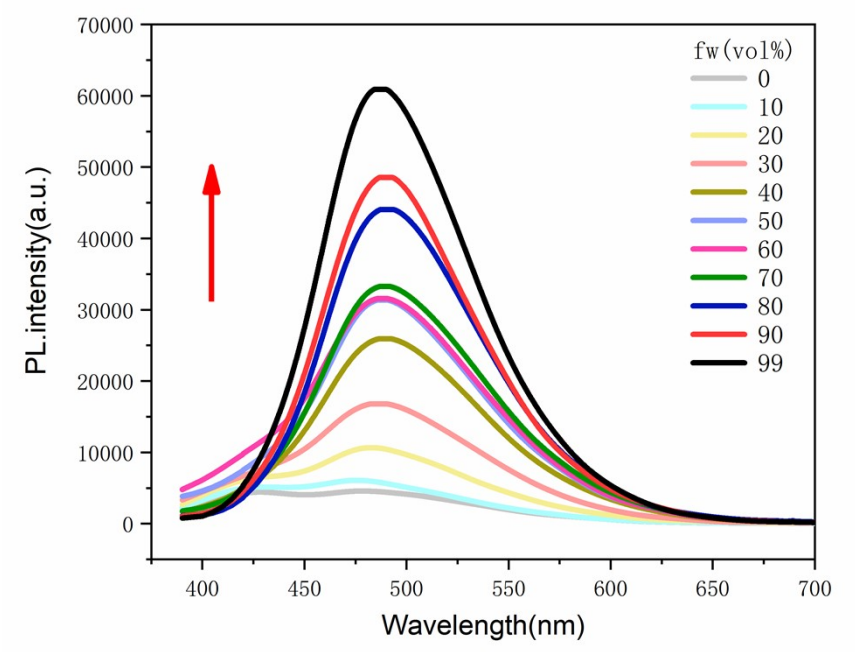

Figure S42. Fluorescence emission Spectrum of **P18.**

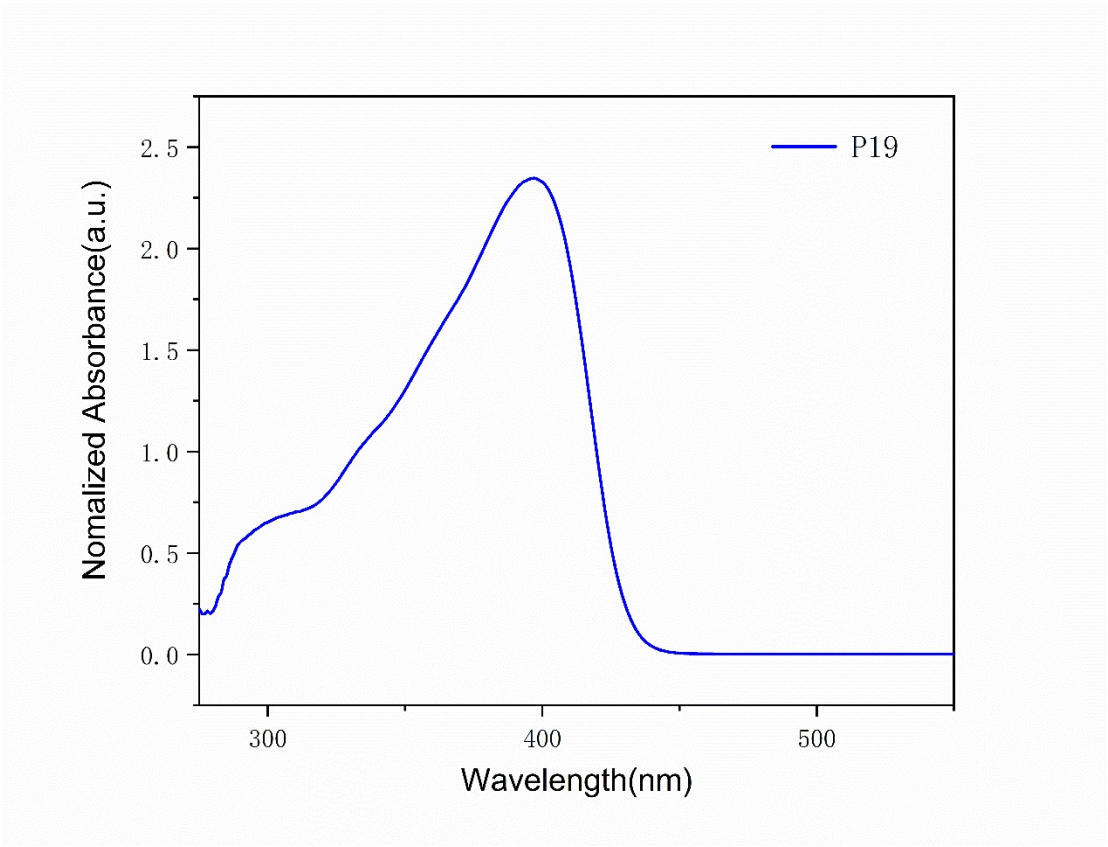

Figure S43. UV-Vis absorption spectrum of **P19.**

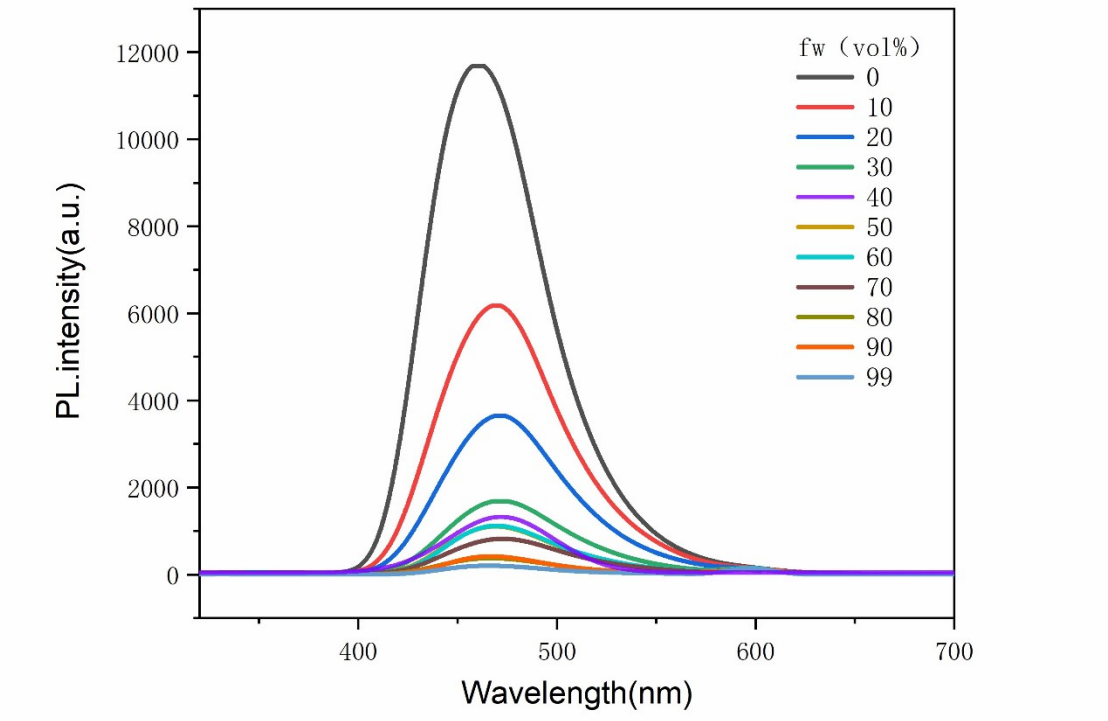

Figure S44. Fluorescence emission Spectrum of **P19.**

5. GPC spectra for the products

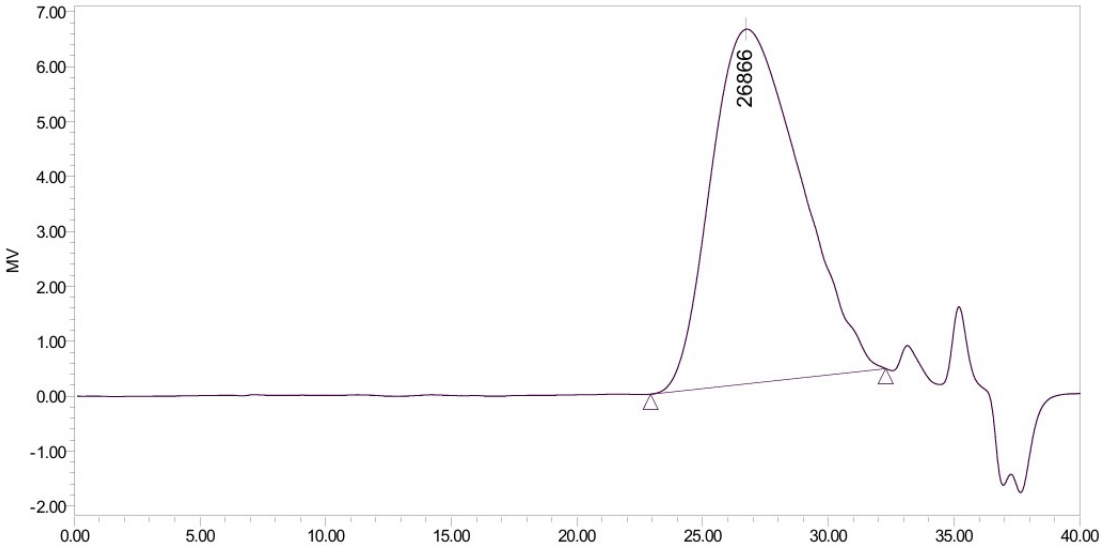

Broad Unknown Relative Peak Table

	Distribution Name	Mn (Daltons)	Mw (Daltons)	MP (Daltons)	Mz (Daltons)	Mz+1 (Daltons)	Polydispersity	Mz/Mw	Mz+1/Mw
1		12528	27569	26866	47518	67559	2.200489	1.723619	2.450592

Figure S45. The GPC spectrum of **P1（C1）**

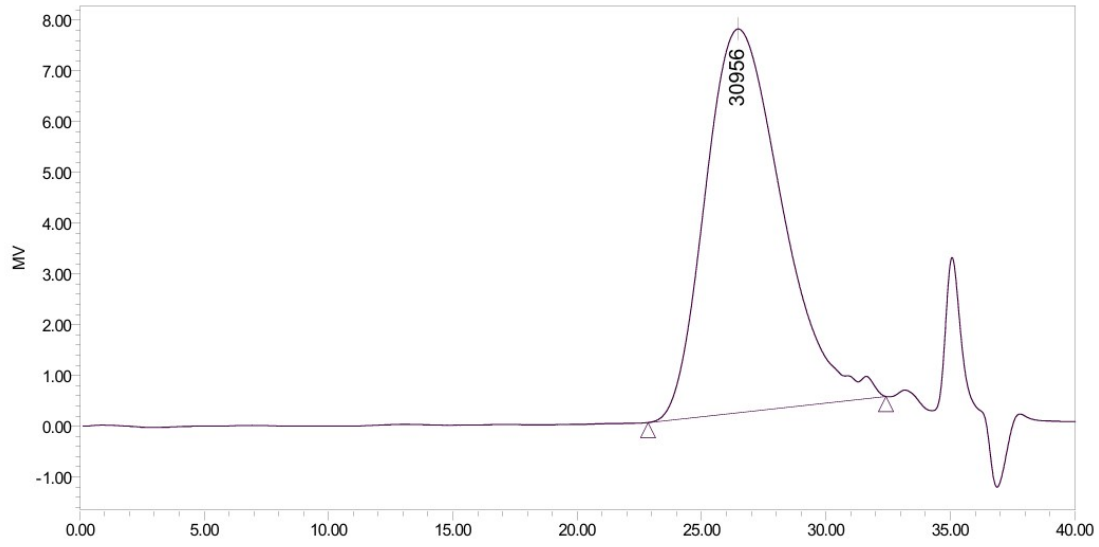

Broad Unknown Relative Peak Table

	Distribution Name	Mn (Daltons)	Mw (Daltons)	MP (Daltons)	Mz (Daltons)	Mz+1 (Daltons)	Polydispersity	Mz/Mw	Mz+1/Mw
1		15643	32984	30956	52584	72404	2.108524	1.594230	2.195129

Figure S46. The GPC spectrum of **P1（C2）**

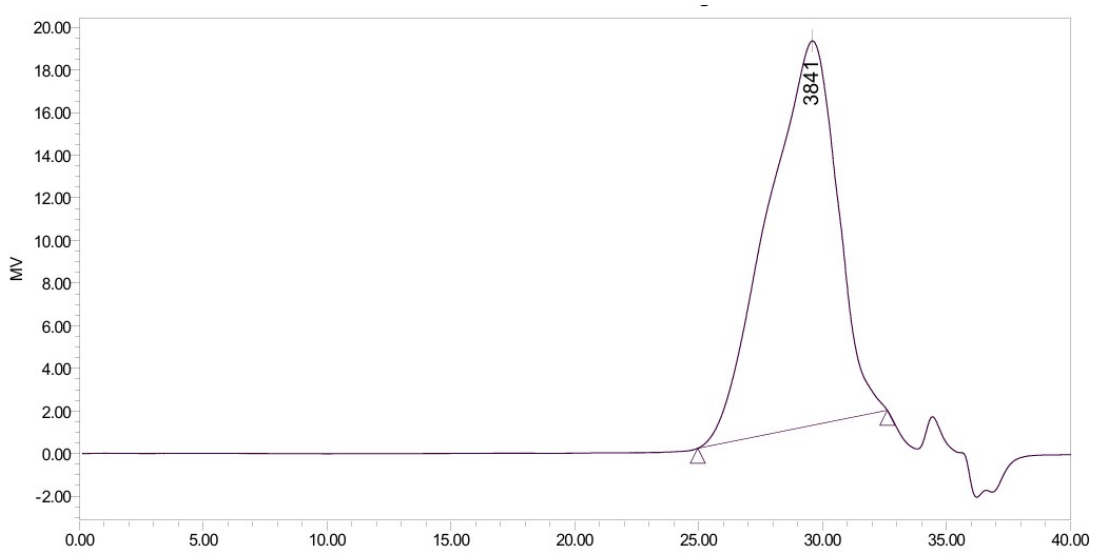

Broad Unknown Relative Peak Table

	Distribution Name	Mn (Daltons)	Mw (Daltons)	MP (Daltons)	Mz (Daltons)	Mz+1 (Daltons)	Polydispersity	Mz/Mw	Mz+1/Mw
1		4048	7061	3841	12289	18628	1.744290	1.740357	2.638068

Figure S47. The GPC spectrum of **P1（C3）**

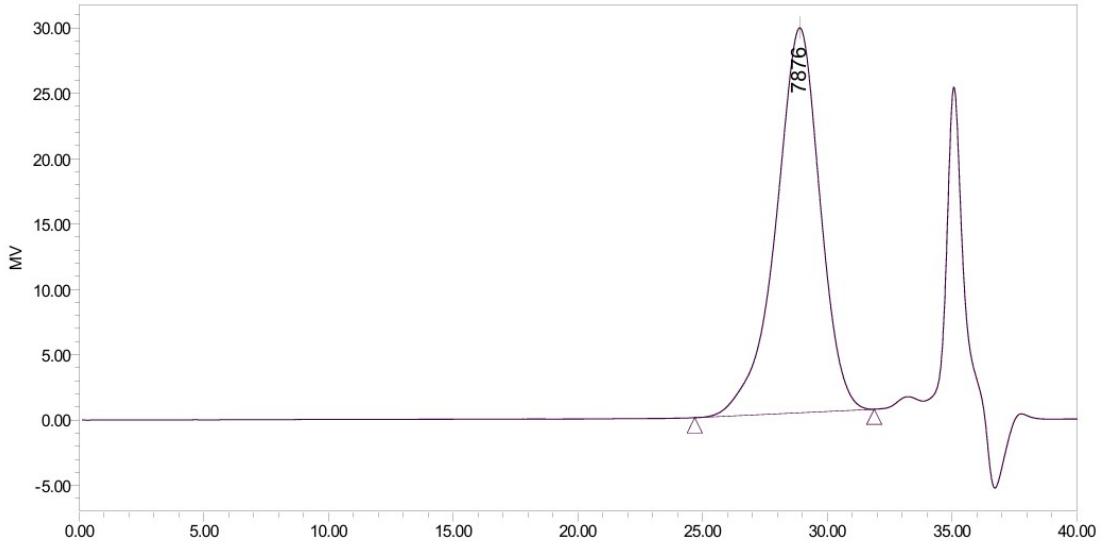

Broad Unknown Relative Peak Table

	Distribution Name	Mn (Daltons)	Mw (Daltons)	MP (Daltons)	Mz (Daltons)	Mz+1 (Daltons)	Polydispersity	Mz/Mw	Mz+1/Mw
1		7458	9717	7876	13424	19394	1.302900	1.381558	1.995951

Figure S48. The GPC spectrum of **P1（C4）**

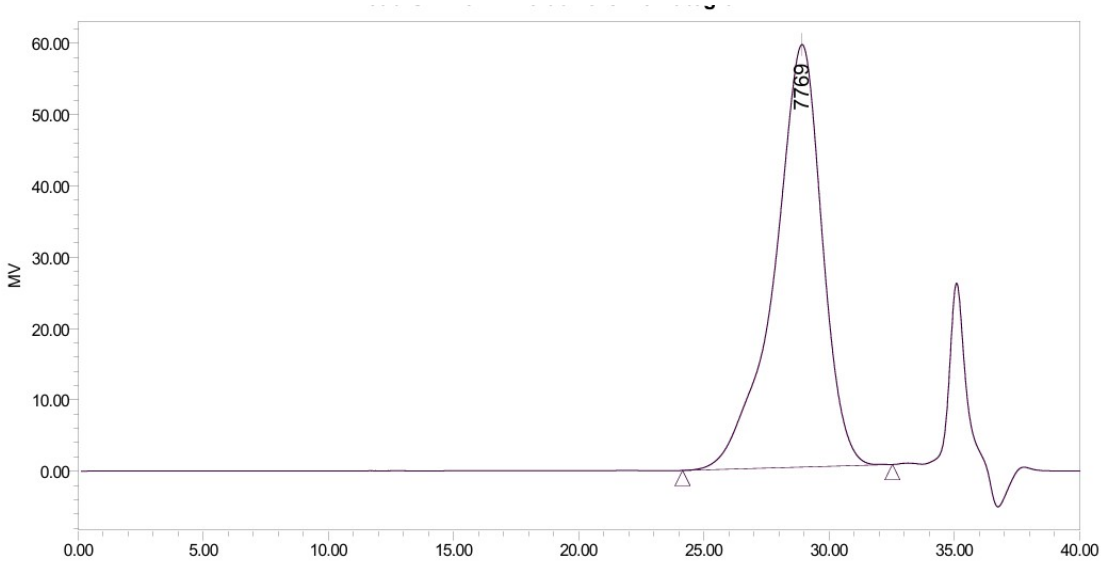

Broad Unknown Relative Peak Table

	Distribution Name	Mn (Daltons)	Mw (Daltons)	MP (Daltons)	Mz (Daltons)	Mz+1 (Daltons)	Polydispersity	Mz/Mw	Mz+1/Mw
1		7759	10859	7769	16696	26259	1.399627	1.537502	2.418143

Figure S49. The GPC spectrum of **P1（C5）**

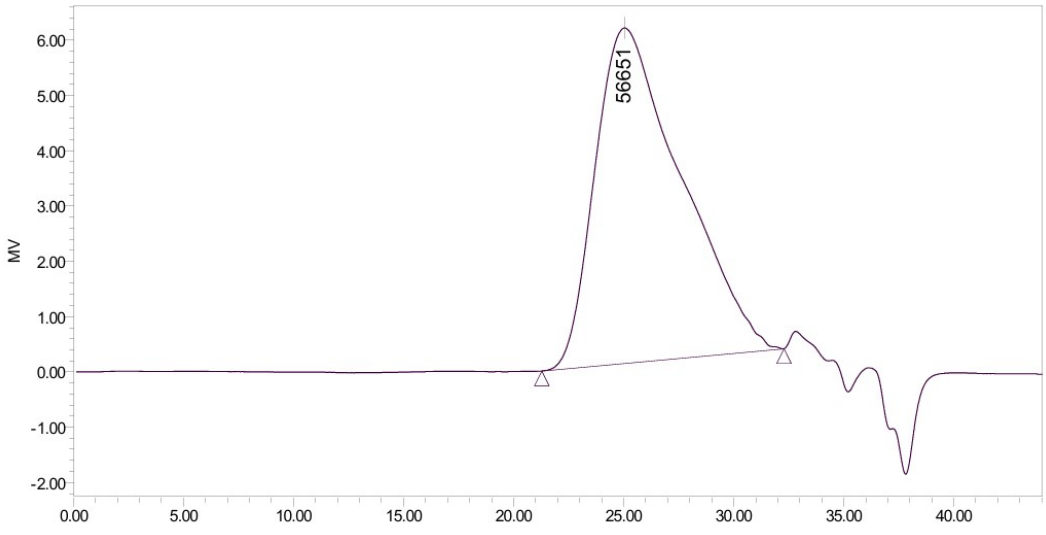

Broad Unknown Relative Peak Table

	Distribution Name	Mn (Daltons)	Mw (Daltons)	MP (Daltons)	Mz (Daltons)	Mz+1 (Daltons)	Polydispersity	Mz/Mw	Mz+1/Mw
1		17771	5011[illegible]	56651	89602	127057	2.819876	1.788050	2.535490

Figure S50. The GPC spectrum of **P2**

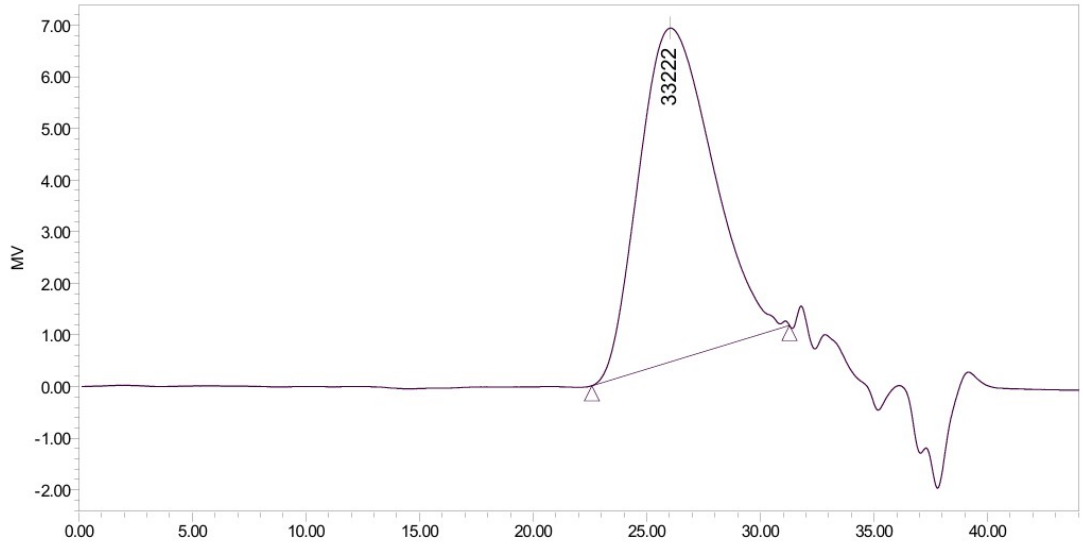

Broad Unknown Relative Peak Table

	Distribution Name	Mn (Daltons)	Mw (Daltons)	MP (Daltons)	Mz (Daltons)	Mz+1 (Daltons)	Polydispersity	Mz/Mw	Mz+1/Mw
1		18890	35259	33222	54421	73278	1.866523	1.543469	2.078290

Figure S51. The GPC spectrum of **P3**

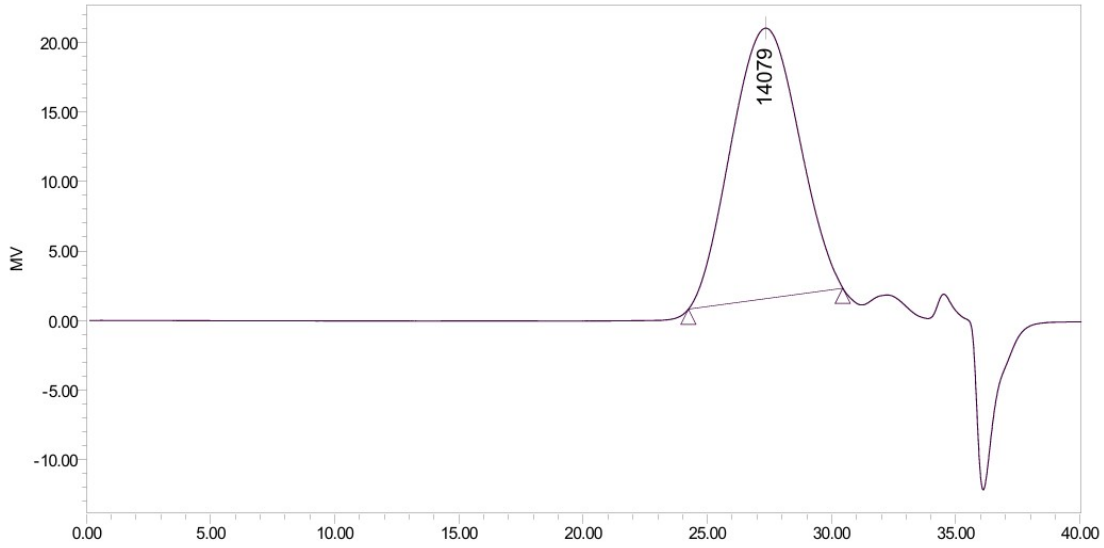

Broad Unknown Relative Peak Table

	Distribution Name	Mn (Daltons)	Mw (Daltons)	MP (Daltons)	Mz (Daltons)	Mz+1 (Daltons)	Polydispersity	Mz/Mw	Mz+1/Mw
1		11296	17657	14079	26165	35114	1.563121	1.481869	1.988736

Figure S52. The GPC spectrum of **P4**

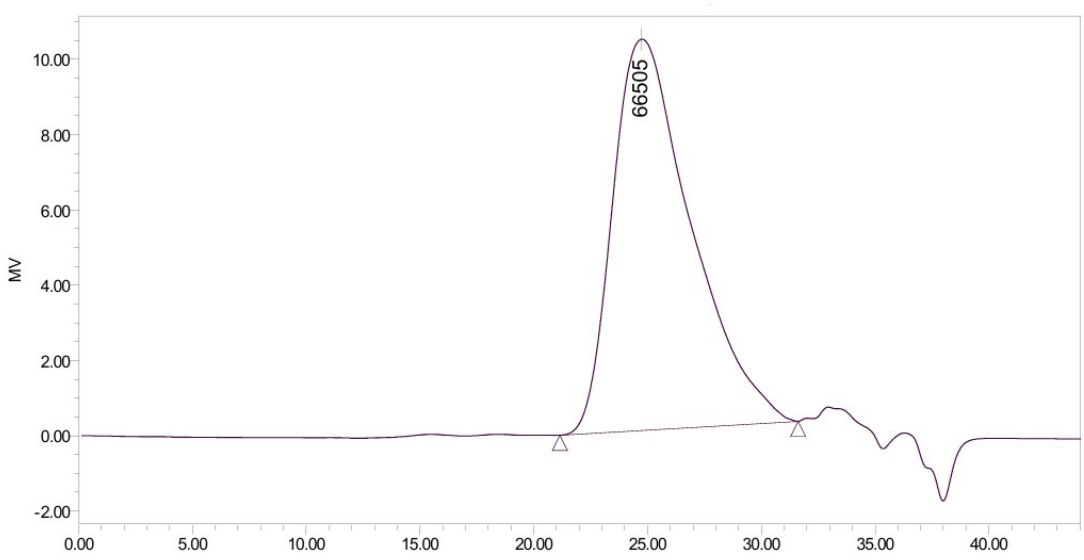

Broad Unknown Relative Peak Table

	Distribution Name	Mn (Daltons)	Mw (Daltons)	MP (Daltons)	Mz (Daltons)	Mz+1 (Daltons)	Polydispersity	Mz/Mw	Mz+1/Mw
1		26214	61365	66505	100315	138154	2.340957	1.634719	2.251332

Figure S53. The GPC spectrum of **P5**

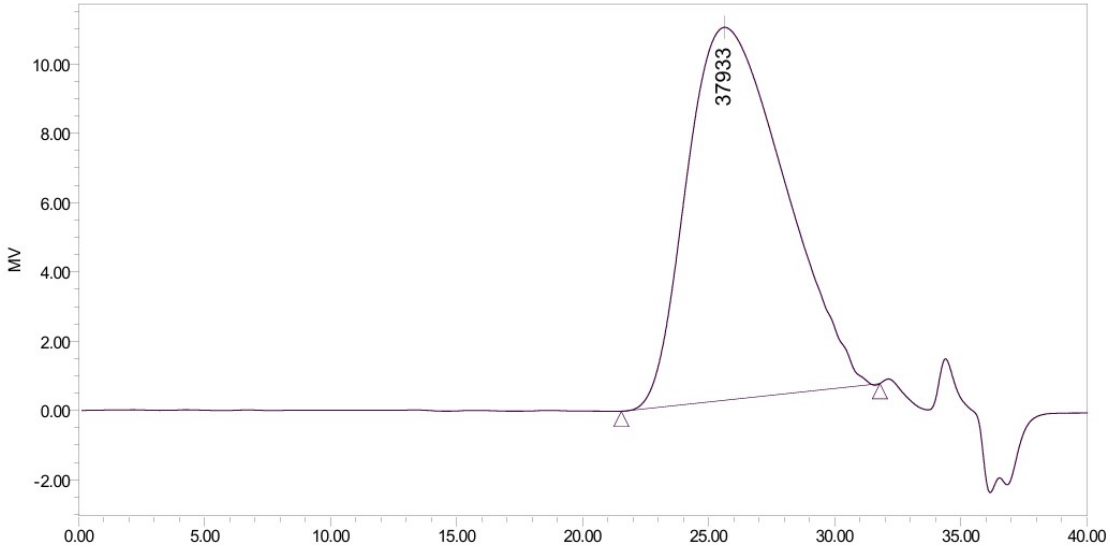

Broad Unknown Relative Peak Table

	Distribution Name	Mn (Daltons)	Mw (Daltons)	MP (Daltons)	Mz (Daltons)	Mz+1 (Daltons)	Polydispersity	Mz/Mw	Mz+1/Mw
1		15255	39228	37933	72476	104952	2.571580	1.847544	2.675406

Figure S54. The GPC spectrum of **P6**

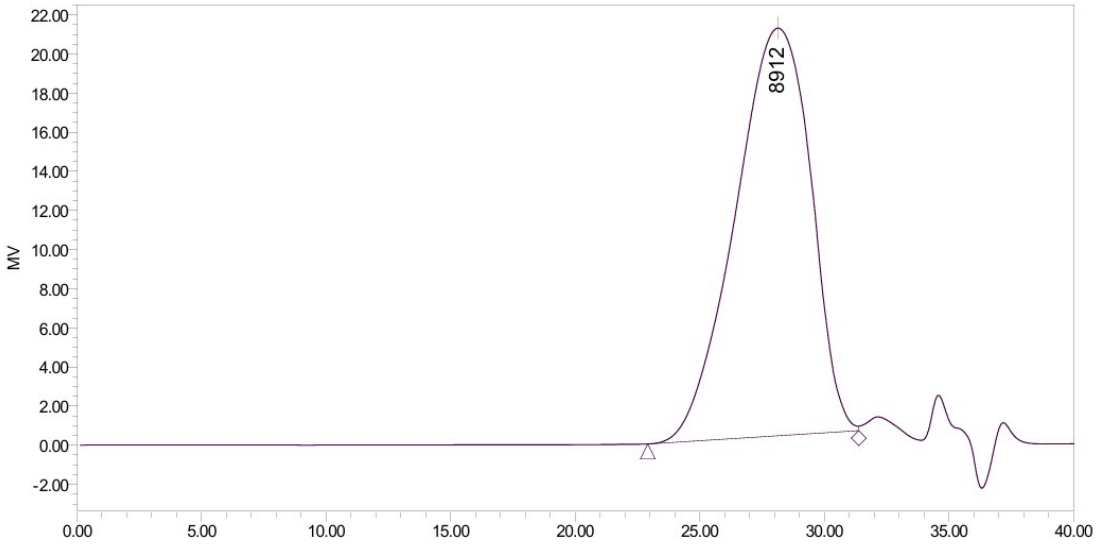

Broad Unknown Relative Peak Table

	Distribution Name	Mn (Daltons)	Mw (Daltons)	MP (Daltons)	Mz (Daltons)	Mz+1 (Daltons)	Polydispersity	Mz/Mw	Mz+1/Mw
1		8033	14461	8912	26958	44379	1.800219	1.864209	3.068963

Figure S55. The GPC spectrum of **P7**

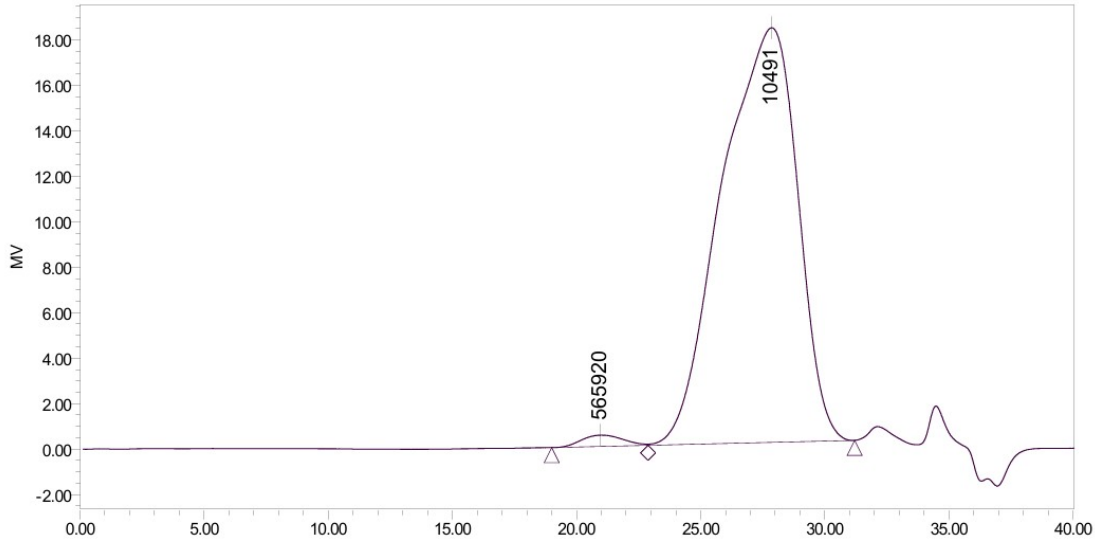

Broad Unknown Relative Peak Table

	Distribution Name	Mn (Daltons)	Mw (Daltons)	MP (Daltons)	Mz (Daltons)	Mz+1 (Daltons)	Polydispersity	Mz/Mw	Mz+1/Mw
1		487489	577857	565920	674469	770040	1.185376	1.167189	1.332579
2		11379	20113	10491	35364	54817	1.767517	1.758281	2.725427

Figure S56. The GPC spectrum of **P8**

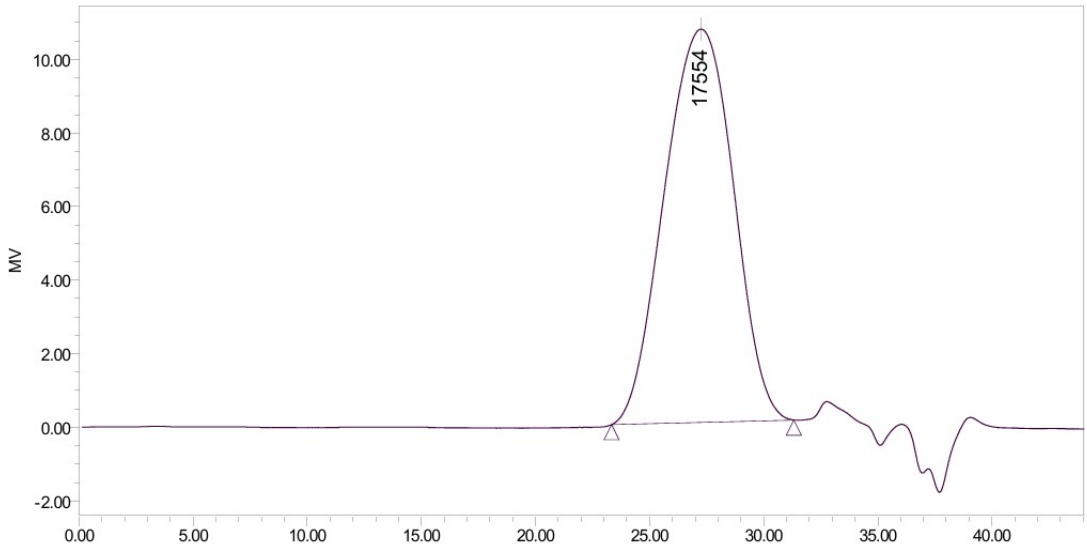

Broad Unknown Relative Peak Table

	Distribution Name	Mn (Daltons)	Mw (Daltons)	MP (Daltons)	Mz (Daltons)	Mz+1 (Daltons)	Polydispersity	Mz/Mw	Mz+1/Mw
1		14130	23093	17554	35454	49245	1.634337	1.535262	2.132442

Figure S57. The GPC spectrum of **P9**

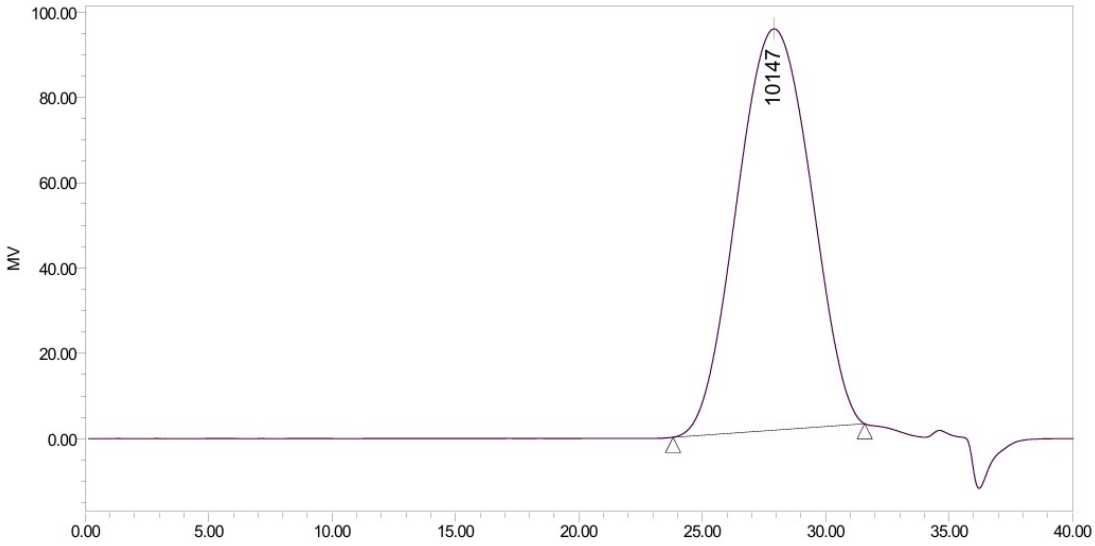

Broad Unknown Relative Peak Table

	Distribution Name	Mn (Daltons)	Mw (Daltons)	MP (Daltons)	Mz (Daltons)	Mz+1 (Daltons)	Polydispersity	Mz/Mw	Mz+1/Mw
1		7705	13283	10147	21811	32015	1.723964	1.642041	2.410300

Figure S58. The GPC spectrum of **P11**

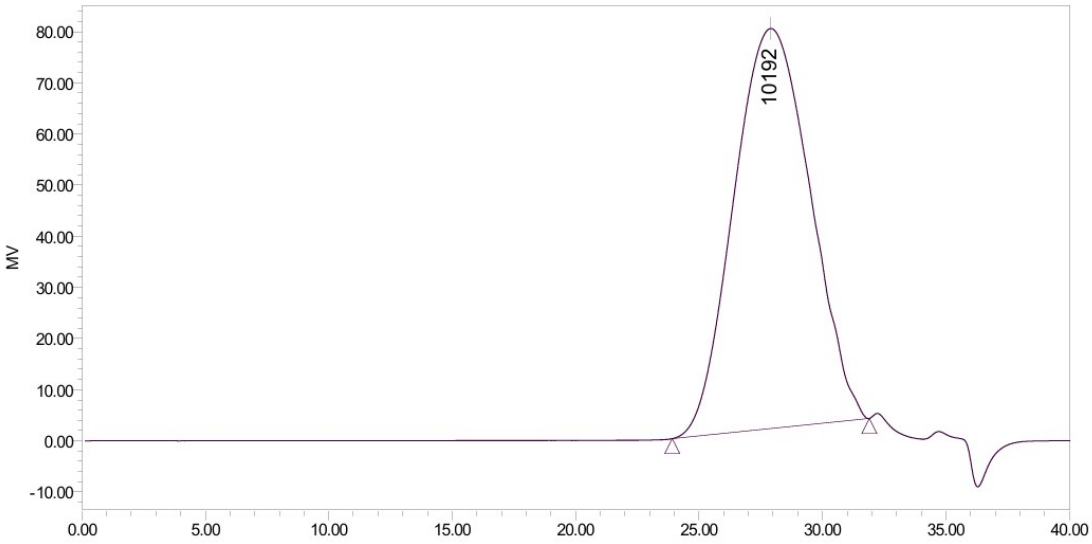

Broad Unknown Relative Peak Table

	Distribution Name	Mn (Daltons)	Mw (Daltons)	MP (Daltons)	Mz (Daltons)	Mz+1 (Daltons)	Polydispersity	Mz/Mw	Mz+1/Mw
1		7154	12890	10192	21369	3111	1.801786	1.657742	2.413787

Figure S59. The GPC spectrum of **P12**

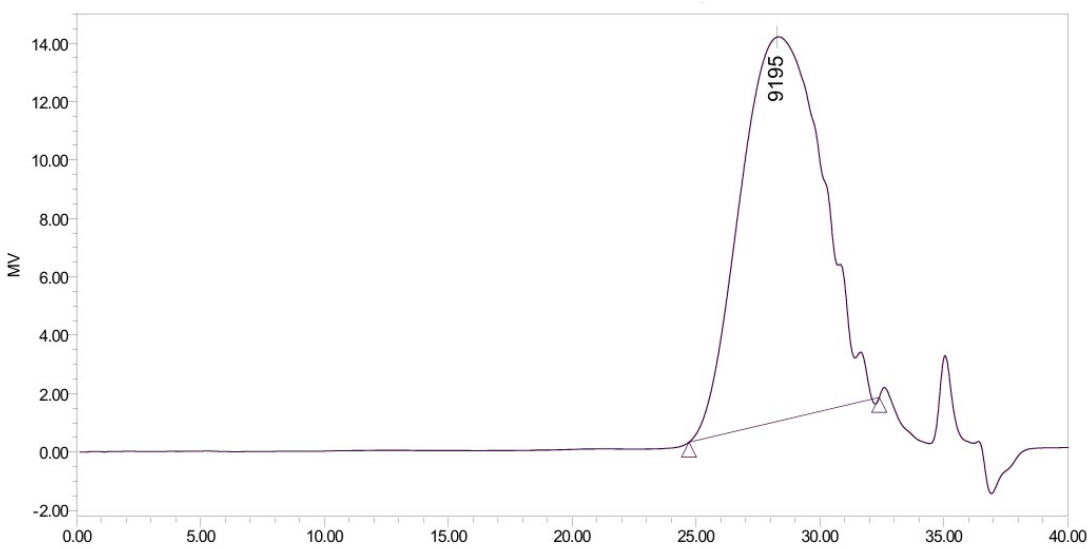

Broad Unknown Relative Peak Table

	Distribution Name	Mn (Daltons)	Mw (Daltons)	MP (Daltons)	Mz (Daltons)	Mz+1 (Daltons)	Polydispersity	Mz/Mw	Mz+1/Mw
1		6169	10823	9195	17553	24782	1.754512	1.621856	2.289726

Figure S60. The GPC spectrum of **P13**

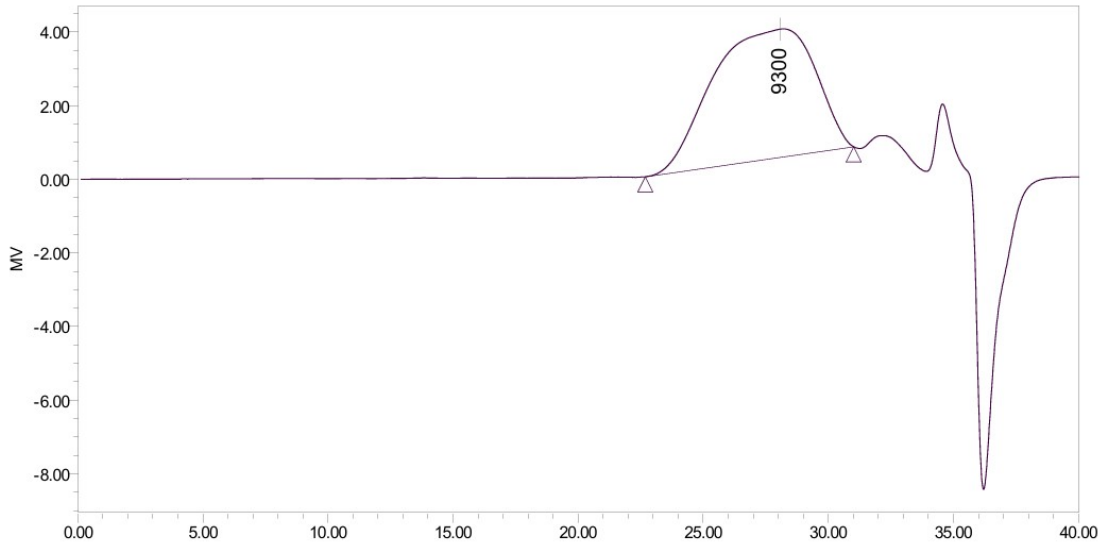

Broad Unknown Relative Peak Table

	Distribution Name	Mn (Daltons)	Mw (Daltons)	MP (Daltons)	Mz (Daltons)	Mz+1 (Daltons)	Polydispersity	Mz/Mw	Mz+1/Mw
1		9828	22043	9300	43346	65397	2.242907	1.966389	2.966726

Figure S61. The GPC spectrum of **P14**

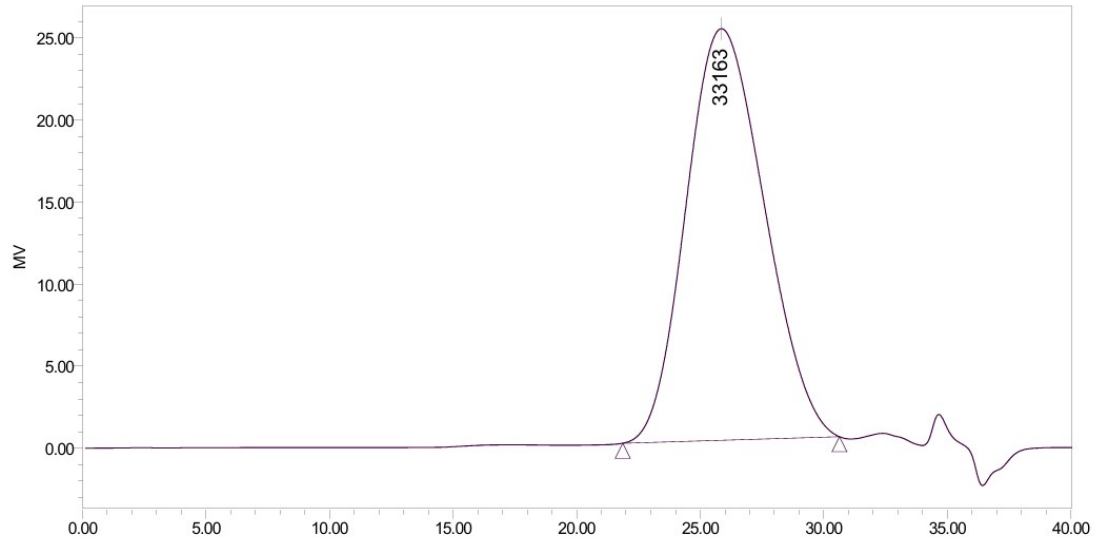

Broad Unknown Relative Peak Table

	Distribution Name	Mn (Daltons)	Mw (Daltons)	MP (Daltons)	Mz (Daltons)	Mz+1 (Daltons)	Polydispersity	Mz/Mw	Mz+1/Mw
1		20219	39219	33163	66782	98988	1.939734	1.702823	2.523998

Figure S62. The GPC spectrum of **P15**

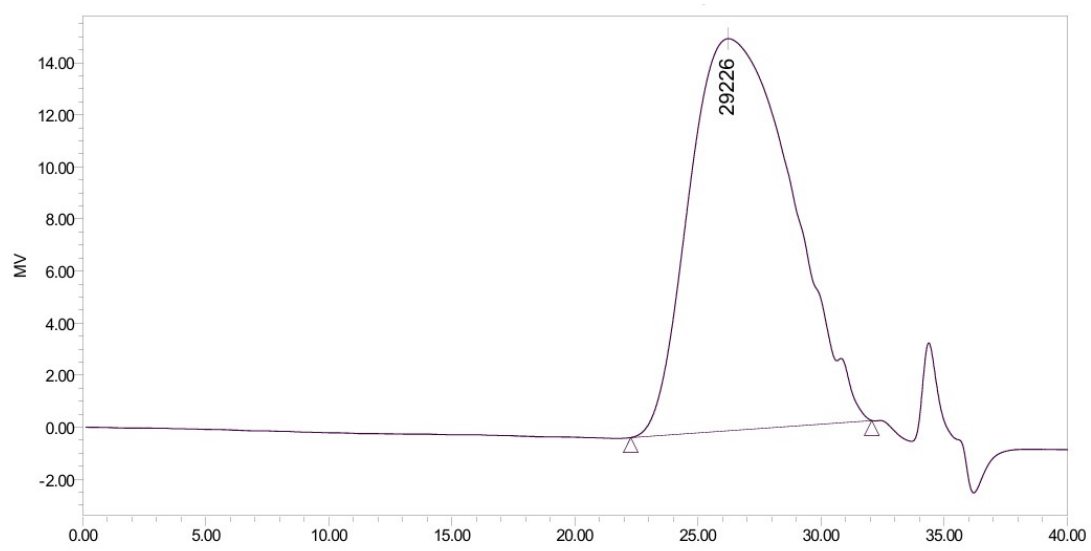

Broad Unknown Relative Peak Table

	Distribution Name	Mn (Daltons)	Mw (Daltons)	MP (Daltons)	Mz (Daltons)	Mz+1 (Daltons)	Polydispersity	Mz/Mw	Mz+1/Mw
1		11995	30299	29226	58262	86791	2.526013	1.922924	2.864511

Figure S63. The GPC spectrum of P**16**

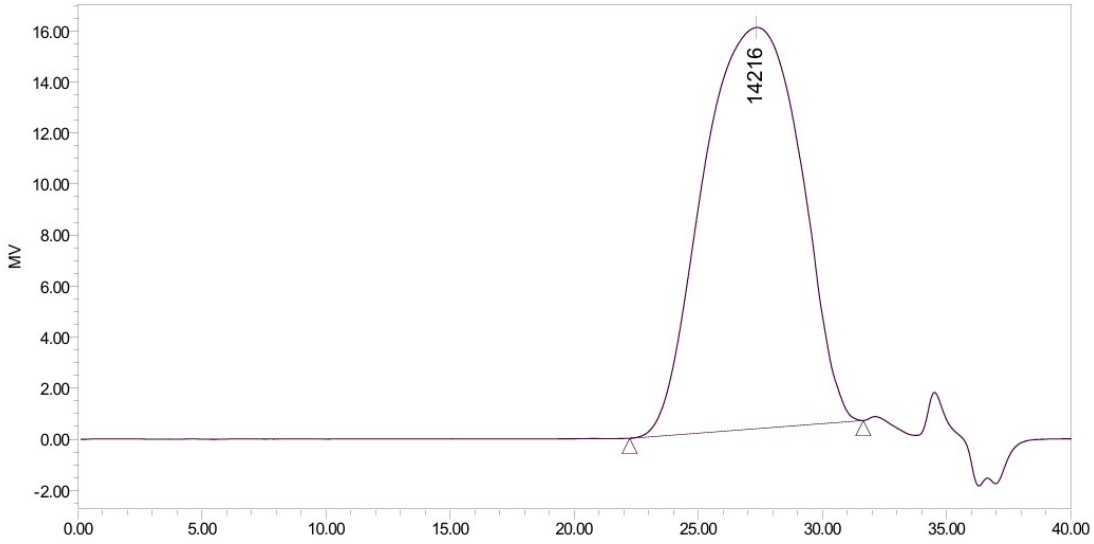

Broad Unknown Relative Peak Table

	Distribution Name	Mn (Daltons)	Mw (Daltons)	MP (Daltons)	Mz (Daltons)	Mz+1 (Daltons)	Polydispersity	Mz/Mw	Mz+1/Mw
1		10591	23623	14216	46147	71248	2.230516	1.953440	3.015994

Figure S64. The GPC spectrum of **P17**

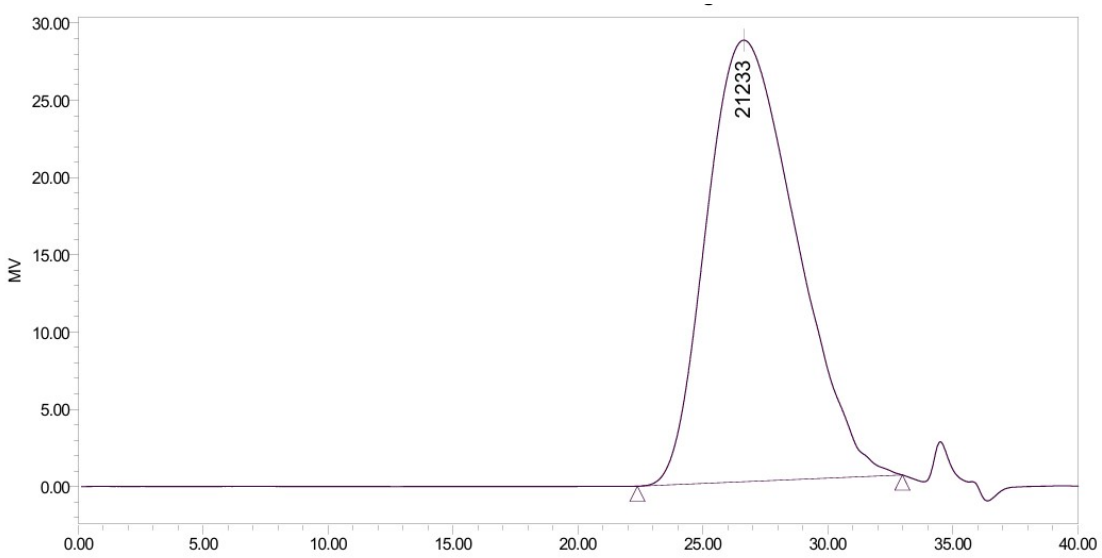

Broad Unknown Relative Peak Table

	Distribution Name	Mn (Daltons)	Mw (Daltons)	MP (Daltons)	Mz (Daltons)	Mz+1 (Daltons)	Polydispersity	Mz/Mw	Mz+1/Mw
1		9688	23318	21233	41981	61696	2.406931	1.800360	2.645810

Figure S65. The GPC spectrum of **P18**

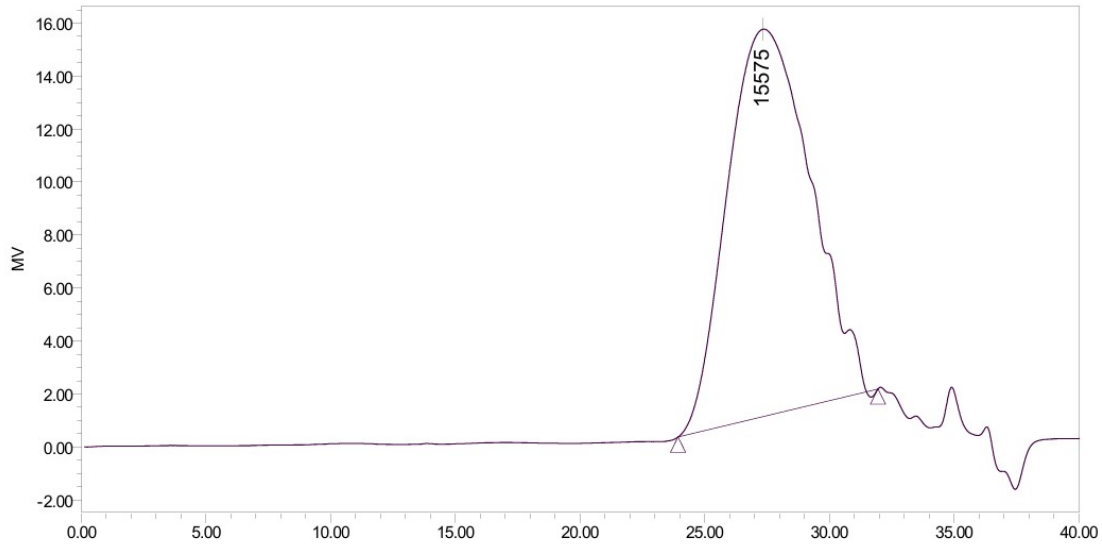

Broad Unknown Relative Peak Table

	Distribution Name	Mn (Daltons)	Mw (Daltons)	MP (Daltons)	Mz (Daltons)	Mz+1 (Daltons)	Polydispersity	Mz/Mw	Mz+1/Mw
1		9324	17259	15575	28117	39238	1.851036	1.629162	2.273520

Figure S66. The GPC spectrum of **P19**

6. DFT calculations of rotational barriers.

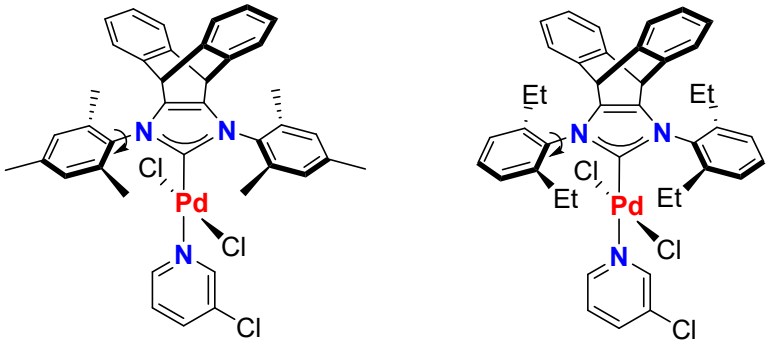

C1
ΔG: 60.4 kcal/mol

C2
ΔG: 58.7 kcal/mol

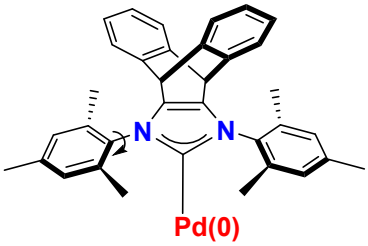

C1'
ΔG: 60.4 kcal/mol

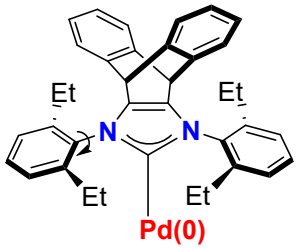

C2'
ΔG: 58.3 kcal/mol

Figure S67. DFT calculations of rotational barriers.

Table S1. DFT calculations of rotational barriers.

Cat.	ΔG (kcal/mol)
C1	60.4
C2	58.7
C1'	60.4
C2'	58.3

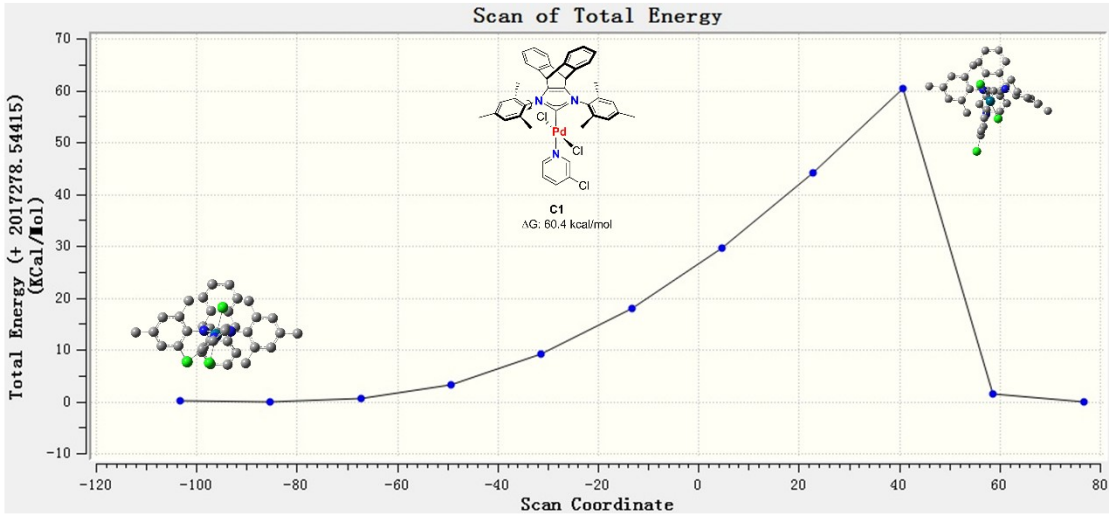

Figure S68. DFT calculations of C_{Ar}–N bond rotation in **C1**.

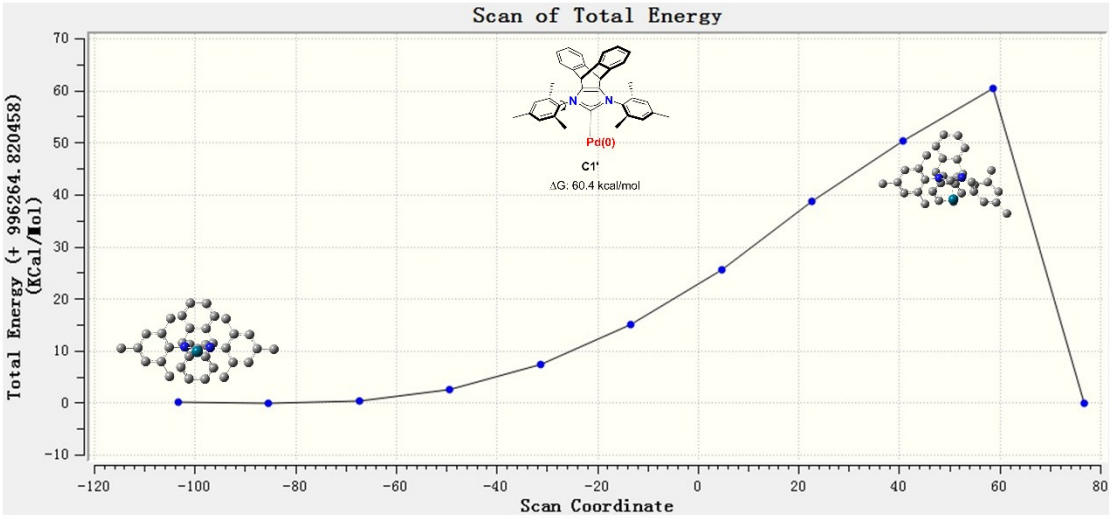

Figure S69. DFT calculations of C_{Ar}–N bond rotation in **C1'**.

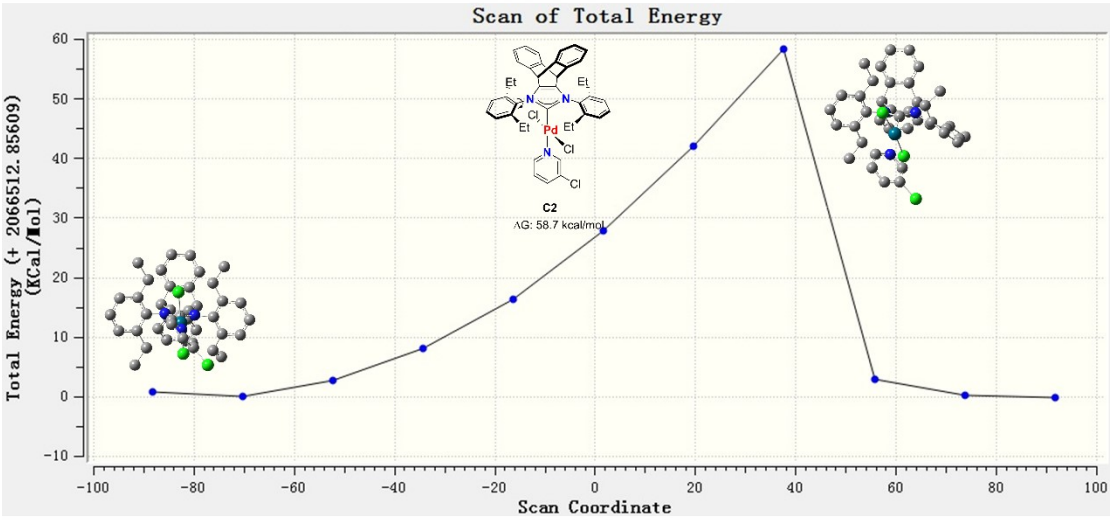

Figure S70. DFT calculations of C_{Ar}-N bond rotation in **C2**.

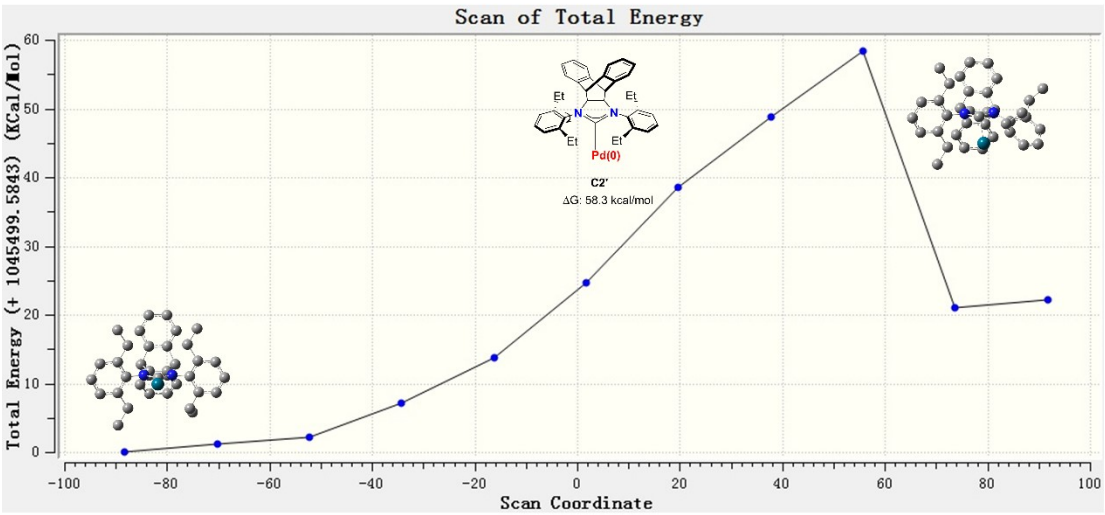

Figure S71. DFT calculations of C_{Ar}-N bond rotation in **C2'**.

Computational details

All the calculation are carried out with the Gaussian 09 program.[1] The structures were optimized in the gas phase by the density functional theory (DFT)[2, 3] with the PBE0 functional and def2-SVP[4,5] basis sets. The C_{Ar}–N bond rotation energies calculations were base on the dihedral angles of C_{Ar} plane and N-N-Pd plane exceeding 180°.

Table S2. Kinetic evaluation of small-molecule model cross-coupling[a]

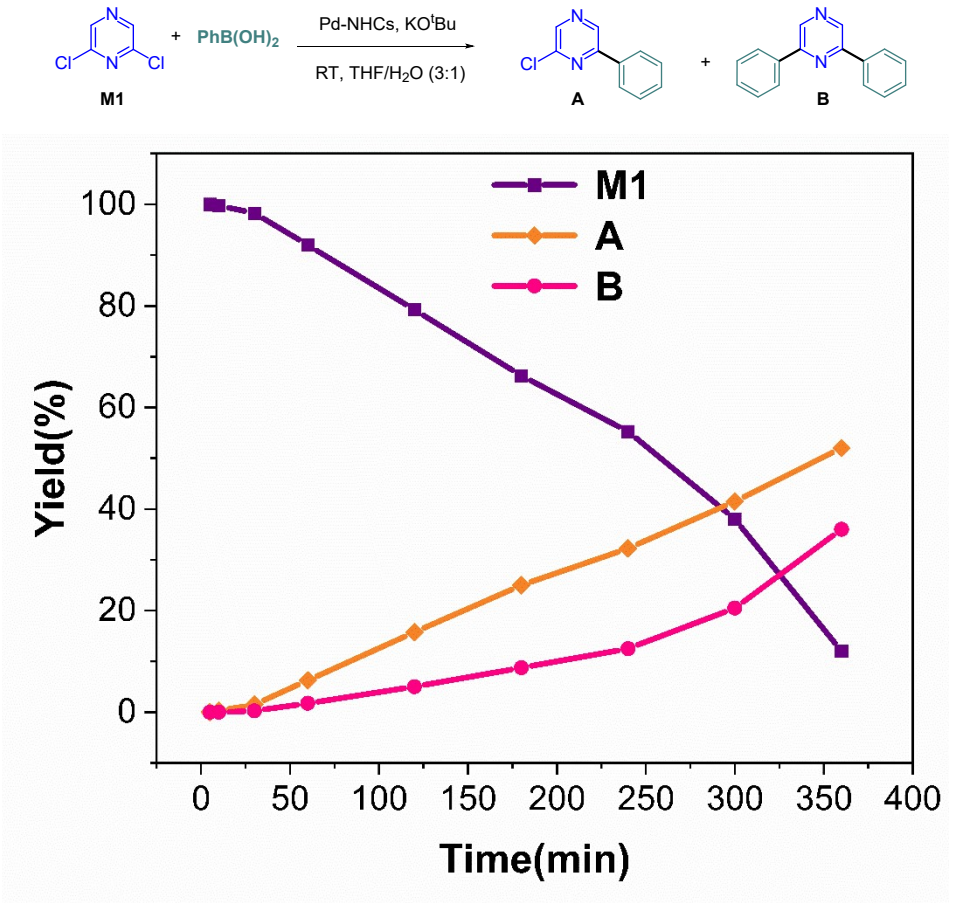

[a] Reaction conditions: 2,6-dichloropyrazine (0.2 mmol), phenylboronic acid (0.2 mmol), THF/H_2O (3:1, 2 mL), KO^{t}Bu (0.4 mmol), Pd-NHC (1 mol%), room temperature (25 °C) for 12 h, under an N_2 atmosphere.

7. Reference

1. Gaussian 09, Revision D.01, M. J. Frisch, G. W. Trucks, H. B. Schlegel, G. E. Scuseria, M. A. Robb, J. R. Cheeseman, G. Scalmani, V. Barone, B. Mennucci, G. A. Petersson, H. Nakatsuji, M. Caricato, X. Li, H. P. Hratchian, A. F. Izmaylov, J. Bloino, G. Zheng, J. L. Sonnenberg, M. Hada, M. Ehara, K. Toyota, R. Fukuda, J. Hasegawa, M. Ishida, T. Nakajima, Y. Honda, O. Kitao, H. Nakai, T. Vreven, J. A. Montgomery, Jr., J. E. Peralta, F. Ogliaro, M. Bearpark, J. J. Heyd, E. Brothers, K. N. Kudin, V. N. Staroverov, T. Keith, R. Kobayashi, J. Normand, K. Raghavachari, A. Rendell, J. C. Burant, S. S. Iyengar, J. Tomasi, M. Cossi, N. Rega, J. M. Millam, M. Klene, J. E. Knox, J. B. Cross, V. Bakken, C. Adamo, J. Jaramillo, R. Gomperts, R. E. Stratmann, O. Yazyev, A. J. Austin, R. Cammi, C. Pomelli, J. W. Ochterski, R. L. Martin, K. Morokuma, V. G. Zakrzewski, G. A. Voth, P. Salvador, J. J. Dannenberg, S. Dapprich,

A. D. Daniels, O. Farkas, J. B. Foresman, J. V. Ortiz, J. Cioslowski, and D. J. Fox, Gaussian, Inc., Wallingford CT, 2013.

2. Kohn, W.; Sham, L. J., Self-Consistent Equations Including Exchange and Correlation Effects. *Physical Review* **1965,** *140* (4A), A1133-A1138.

3. Hohenberg, P.; Kohn, W., Inhomogeneous Electron Gas. *Physical Review* **1964,** *136* (3B), B864-B871.

4. Weigend, F.; Ahlrichs, R., Balanced basis sets of split valence, triple zeta valence and quadruple zeta valence quality for H to Rn: Design and assessment of accuracy. *Phys Chem Chem Phys* **2005,** *7* (18), 3297-305.

5. Weigend, F., Accurate Coulomb-fitting basis sets for H to Rn. *Phys Chem Chem Phys* **2006,** *8* (9), 1057-65.